What are chances for Cassiopeia A being produced by the binary system?

Are there chances for Cassiopeia A to be the result of a binary system evolution?

Anatoly Iyudin

Skobeltsyn Institute of Nuclear Physics,
Moscow State University

"The Progenitor-Supernova-Remnant Connection"
Ringberg, Germany, 24-28 July 2017

Abstract

In this talk we consider in historical perspective observational evidence(s) for the possible scenario of young galactic SNR Cas A to be the result of a binary system evolution.
Historical records and recent observations of this object are used (not) to draw (even) a preliminary conclusion on the Cas A binary progenitor.

Binary progenitors of SN IIb

Smartt (2009)

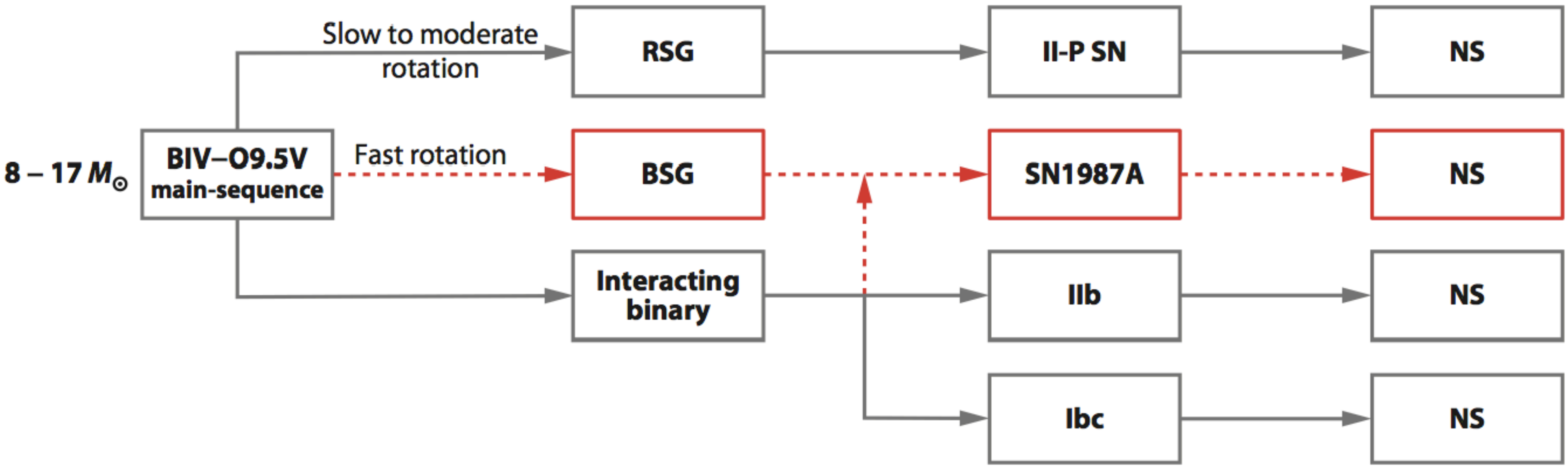

It is sort of a common believe that many SNe IIb are produced by binary systems

Binary and progenitors

Binary Interaction Dominates the Evolution of Massive Stars

H. Sana,[1*] S. E. de Mink,[2,3] A. de Koter,[1,4] N. Langer,[5] C. J. Evans,[6] M. Gieles,[7] E. Gosset,[8] R. G. Izzard,[5] J.-B. Le Bouquin,[9] F. R. N. Schneider[5]

The presence of a nearby companion alters the evolution of massive stars in binary systems, leading to phenomena such as stellar mergers, x-ray binaries, and gamma-ray bursts. Unambiguous constraints on the fraction of massive stars affected by binary interaction were lacking. We simultaneously measured all relevant binary characteristics in a sample of Galactic massive O stars and quantified the frequency and nature of binary interactions. More than 70% of all massive stars will exchange mass with a companion, leading to a binary merger in one-third of the cases. These numbers greatly exceed previous estimates and imply that binary interaction dominates the evolution of massive stars, with implications for populations of massive stars and their supernovae.

Sana et al., Science (2012)

Binary and progenitors

Sana et al. (2012)

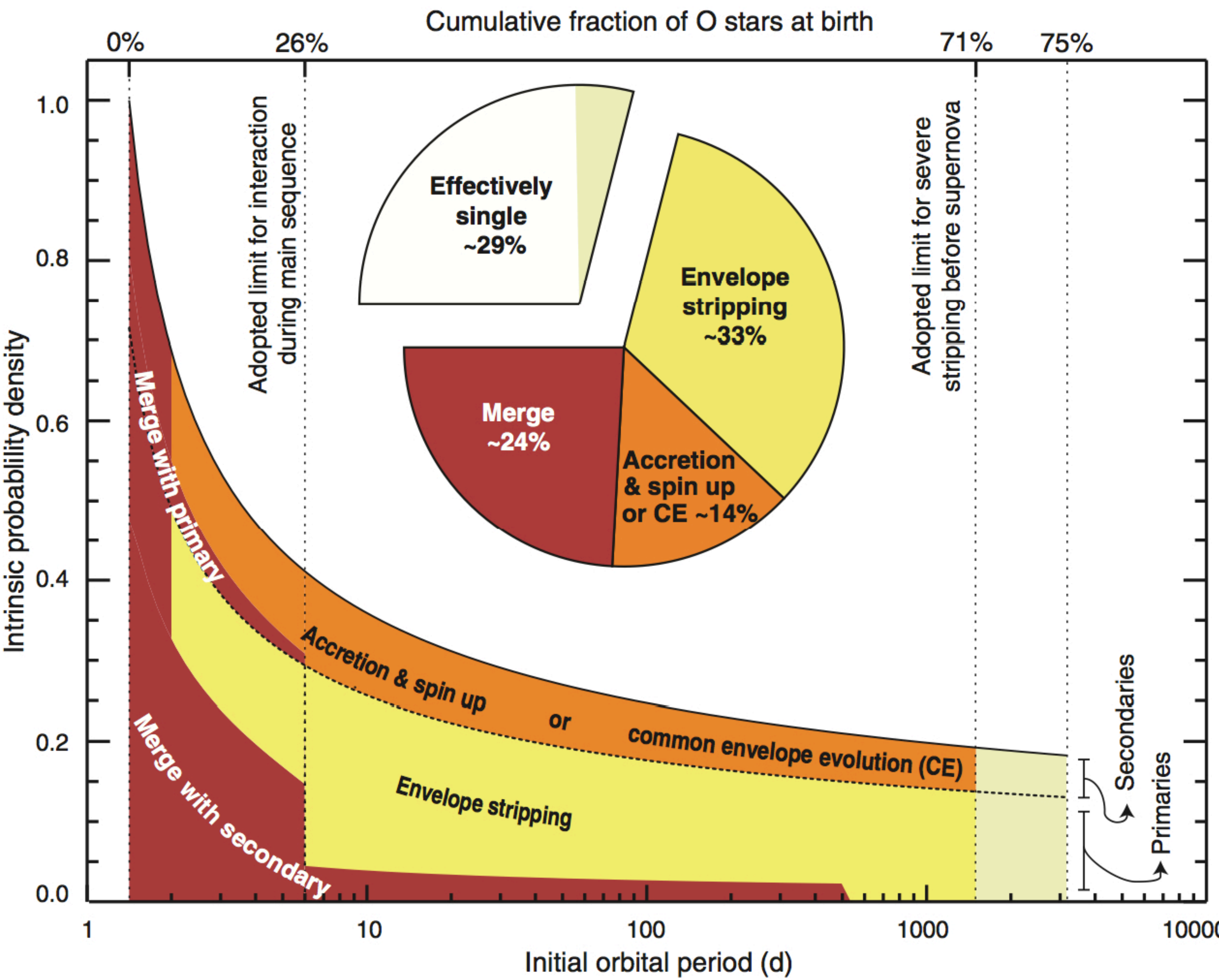

Baade and Minkowski, ApJ, 119, p. 206 (1954)

Position was communicated
In fall of 1951 by F.G. Smith,
Cavendish Laboratory, in advance
of Nature publication of radio results

Measurements by Baade&Minkowski were taken in September 1951, at 200' telescope.

TABLE 1

POSITION OF THE SOURCE IN CASSIOPEIA, RYLE 23.01

α (1950)	δ (1950)	Method	Observer
$23^h21^m12^s \pm 10^s$......	$+58°32' \pm 4'$	Radio interferometer	Ryle, Smith, and Elsmore*
$23^h21^m12\overset{s}{.}0 \pm 1^s$.....	$+58°32\overset{'}{.}1 \pm 0\overset{'}{.}7$	Radio interferometer	Smith†
$23^h21^m36^s \pm 30^s$......	$+58°38' \pm 10'$	Radio paraboloid	R. Hanbury Brown‡
$23^h21^m11\overset{s}{.}38$........	$+58°31'52\overset{''}{.}9$	Photographic	Baade

* *M.N.*, **110**, 508, 1950.
† *Nature*, **168**, 555, 1951.
‡ *M.N.*, **113**, 123, 1953.

First optical observations of Cassiopeia A supernova remnant

Baade and Minkowski, ApJ, 119, p. 206 (1954)

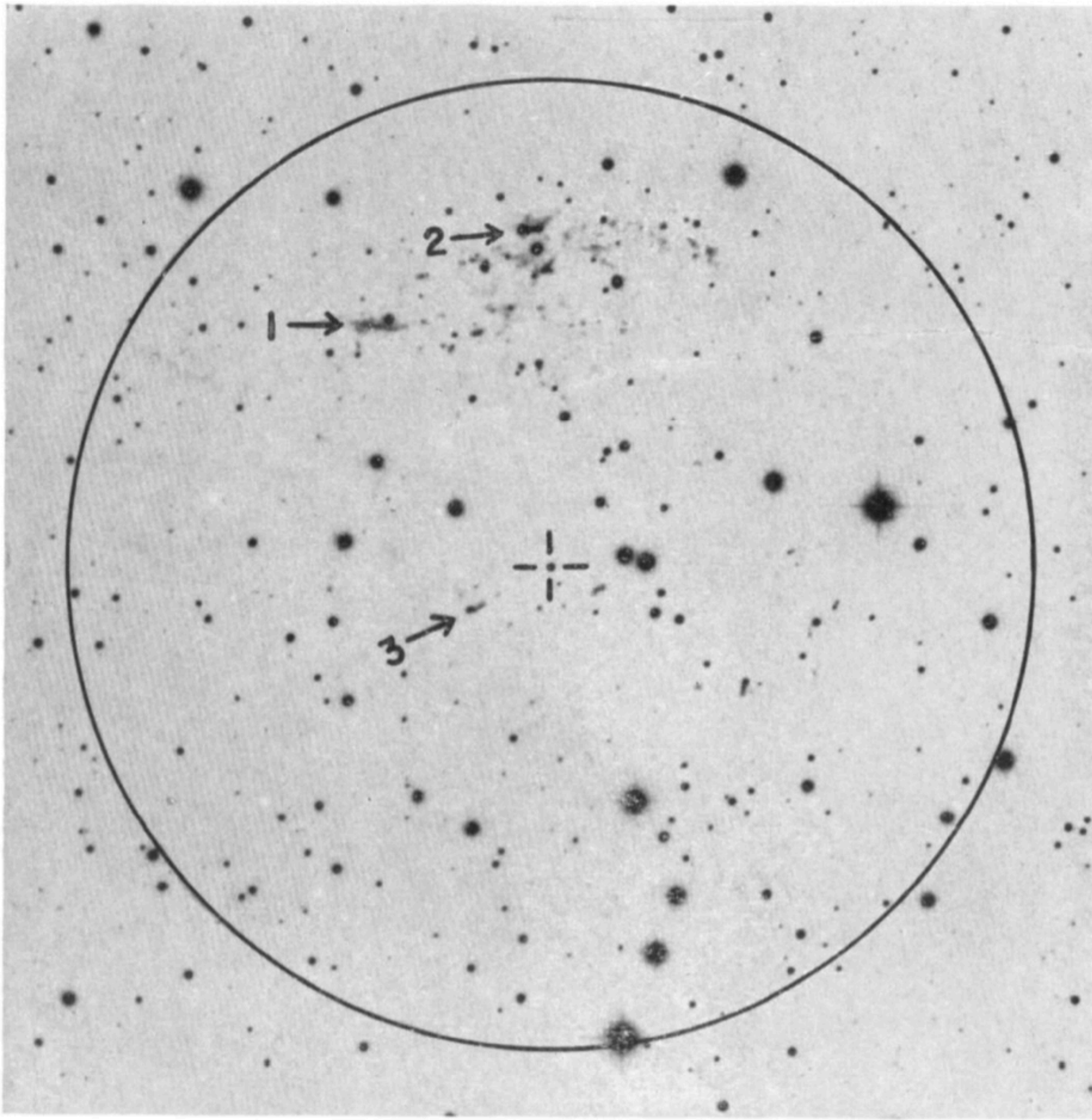

FIG. 3.—Nebulosity in Cassiopeia. λλ 6400–6700; 200-inch; 1 mm = 4″.9

Measurements by Baade&Minkowski were taken in September 1951, at 200' Telescope.

Baade and Minkowski, ApJ, 119, p. 206 (1954)

Although the center of the visible nebulosity closely coincides with a star of photographic magnitude 18.9, there is no reason to identify this star with the exciting source of the nebulosity, since in no way does it stand out by its color. The same is true of the other stars near the center, so that there is no visible source of excitation for the nebulosity.

Obviously, the identification of the radio source with the nebulosity just described would be strengthened very much if it could be shown that the radio source has the same diameter as the visible nebulosity. At our request, F. G. Smith[7] measured the diameter of the Cassiopeia source interferometrically. It turned out that the radio source has indeed a measurable diameter. From his measures Smith derived $d = 5\overset{\prime}{.}6 \pm 0\overset{\prime}{.}2$ under the assumption of a uniformly radiating disk, or $d = 5\overset{\prime}{.}0 \pm 0\overset{\prime}{.}2$ if the shell is optically thin. Observations by Hanbury Brown, Jennison, and Das Gupta[8] indicate a slightly elliptical area of $3' \times 4'$, with the major axis approximately in position angle 25°. The values for the diameter of the radio source are in such good agreement with the diameter of the visible nebulosity that there can be no further doubt about the identification. Both in position and in diameter the two objects agree within the errors of measurements.

Minkowski, IAUS #9, p. 315 (1959)

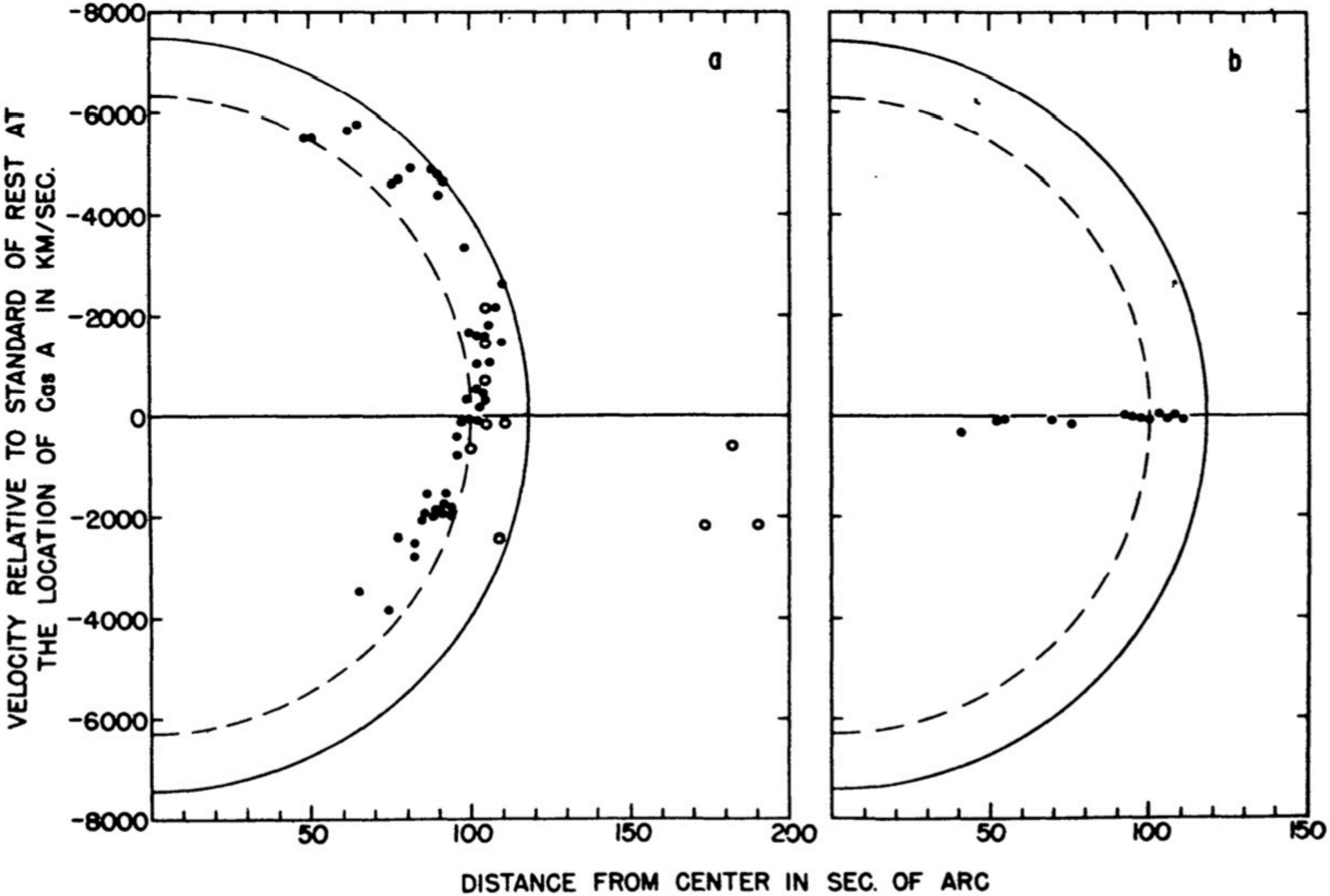

FIG. 4. Radial velocities in Cassiopeia A as function of the distance from the center.

Minkowski, IAUS #9, p. 315 (1959)

TABLE I

POSITIONS OF CASSIOPEIA A

	$\alpha(1950)$	$\delta(1950)$
Center of circular area	$23^h21^m9\overset{s}{.}4$	$+58°32'27''$
Center of expansion	$23^h21^m11\overset{s}{.}8 \pm 0\overset{s}{.}4$	$+58°32'16'' \pm 8''$
Position of source*	$23^h21^m12\overset{s}{.}0 \pm 1^s$	$+58°32\overset{'}{.}1 \pm 0\overset{'}{.}7$

* F. G. Smith, *Nature*, **168**, 555, 1951.

The velocity of expansion of 7440 km/second in combination with the observed motion leads to a distance of 3400 parsecs, with an estimated uncertainty of perhaps 300 parsecs. This value is in excellent agreement with the results derived from the study of the 21 cm absorption lines [10, 11]. At a distance of 3400 parsecs, Cassiopeia A is 140 parsecs south of the galactic plane in a region where Westerhout [12] finds a density of hydrogen atoms of 0.2 cm^{-3}. The linear diameter of the circular nebulosity is 4.0 parsecs.

[10] Hagen, J. P., Lilley, A. E., and McClain, E. F. *Ap. J.* **122**, 361, 1955. *Radio Astronomy* (I.A.U. Symposium No. 4), p. 82.
[11] Muller, C. A. *Ap. J.* **125**, 830, 1957.
[12] Westerhout, G. *B.A.N.* **13**, 201, 1957.

Minkowski, IAUS #9, p. 315 (1959)

Now that the distance of the nebulosity is safely established, the linear size of the condensations and their mass can be stated. Most of the average condensations of both types have apparent diameters of 1 to 2 seconds of arc. With a distance of 3400 parsecs, their linear diameters are 5 to 10×10^{16} cm. The mass of the average fast-moving condensation is then about 2×10^{30}, and the combined mass of the roughly 200 fast-moving condensations thus is about 2×10^{32} grams. Only a fraction of the total shell is visible, however, and the total mass of the complete moving shell would probably be close to 1 solar mass. The average mass of a semistationary condensation is about 10^{32} grams, and the combined mass of the relatively few condensations of this type also amounts to about 1 solar mass, but it seems plausible to assume that this mass was not part of the moving shell, but was gathered in the formation of the semistationary condensations.

There is no longer doubt that the nebulosity is the remnant of a type II supernova. This is the only type of object for which velocities of expansion of the order 5000 km/second have been reported; a value of 7500 km/second is well within the range of possible interpretations. Moreover, no other type of nova or supernova is known to have an ejected mass of the order of 1 solar mass. An ejected mass of this order seems acceptable for the type II

Kamper & van den Bergh (1976)

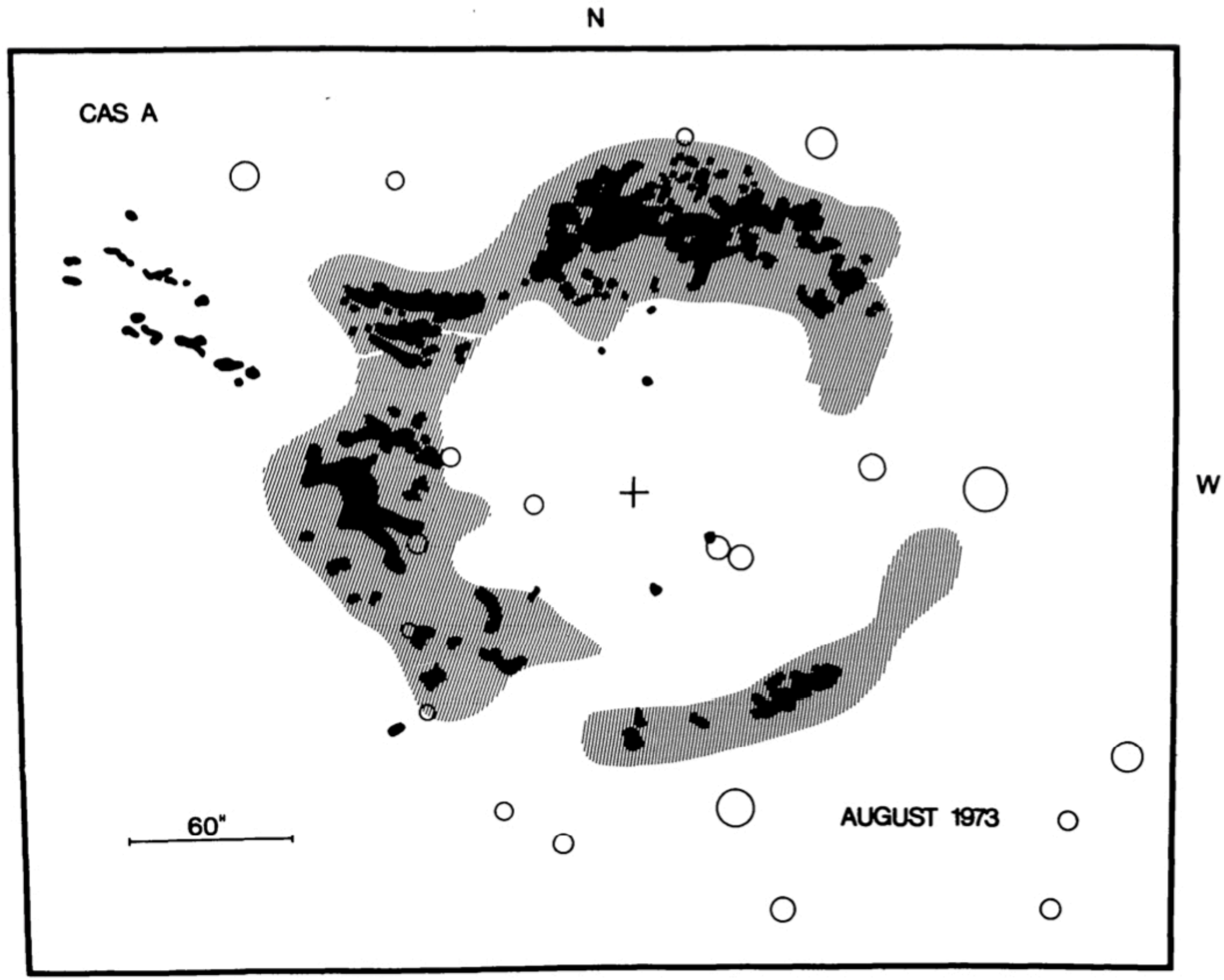

FIG. 2.—Distribution of nebulosity in which [S II] is strong relative to [O III]. The center of expansion of the fast-moving knots is marked by a cross. The ring-shaped region in which faint [S II] emission is marginally visible on a deep interference-filter photograph is also shown. Bright stars are shown as circles.

Kamper & van den Bergh (1976)

COMPARISON OF DETERMINATIONS OF THE

CENTER OF EXPANSION OF CAS A

Author(s)	Period	$\alpha(1950)$	$\delta(1950)$
Minkowski (1959)	1951 - 1954	$23^h21^m11\overset{s}{.}8 \pm 0\overset{s}{.}4$	$+58^\circ 32' 16'' \pm 8''$
van den Bergh and Dodd (1970)	1951 - 1968	23 21 11.4 ± 0.2	+58 32 18.9 ± 3.1
Rosenberg* (1970)	1968	23 21 9.5 ± 0.8	+58 32 22 ± 5
Present study	1951 - 1975	23 21 12.0 ± 0.1	+58 32 17.9 ± 0.8
correcting p.m.		23 21 12.0	+58 32 20.1

* Geometrical center of radio source

Kamper & van den Bergh (1976)

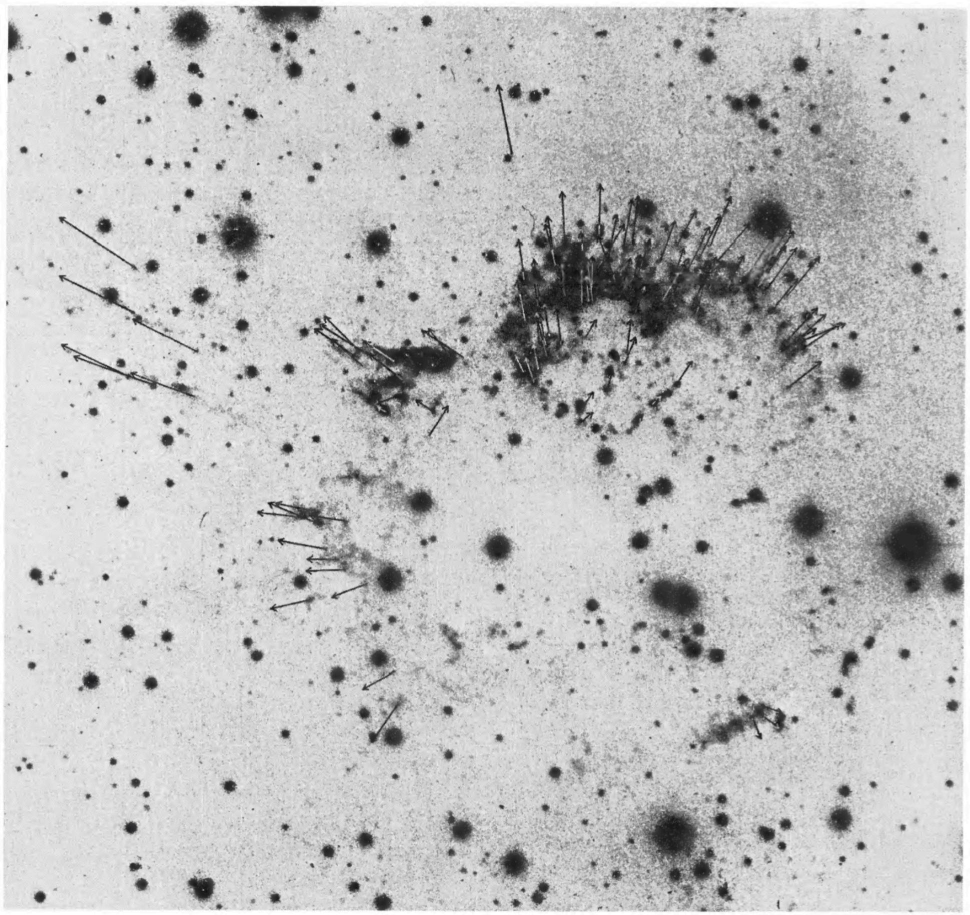

FIG. 8.—Fifty-year proper motion vectors for fast-moving knots plotted on plate PH 6573

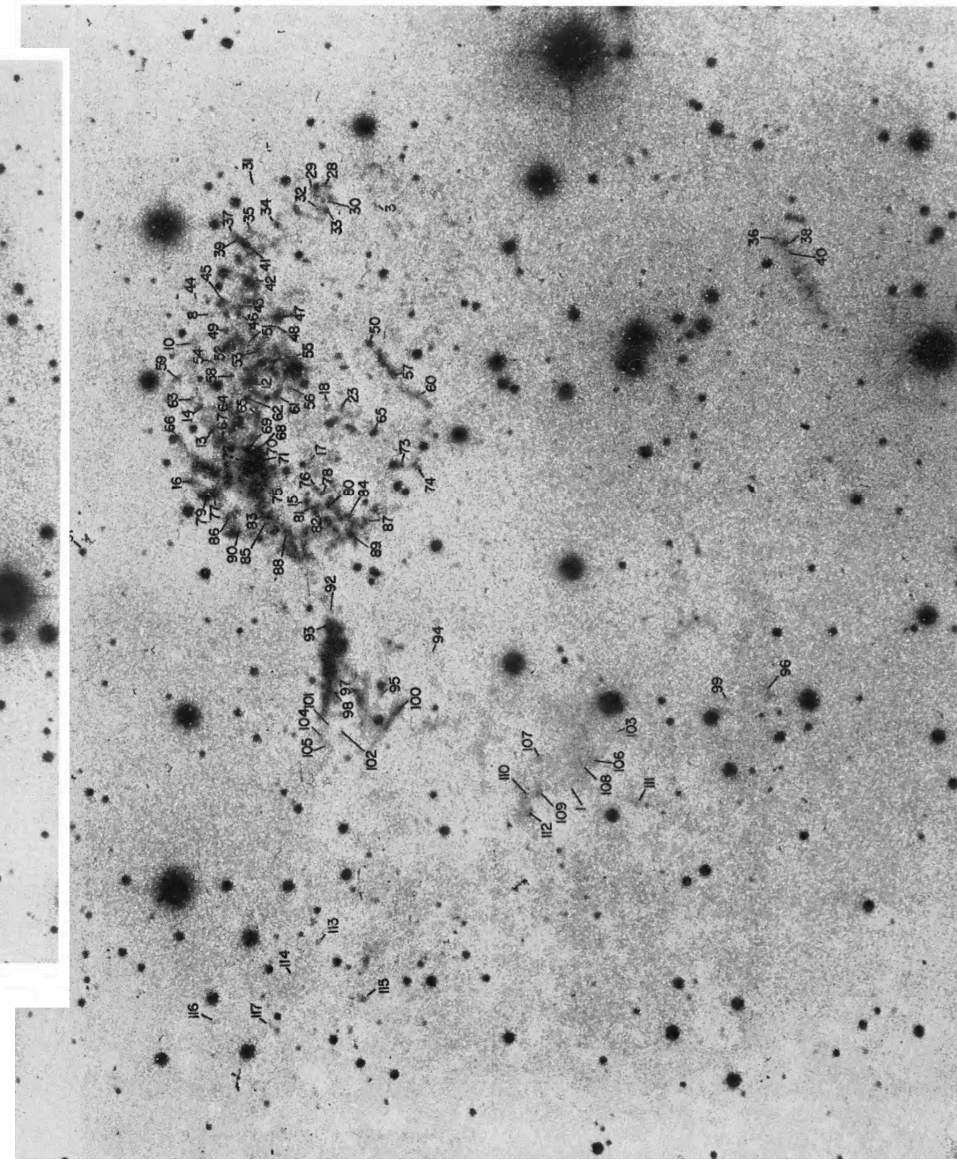

FIG. 7.—Identification chart (PH 6914vB) taken in 1974 for moving knots that are visible on recent plates of Cas A

Kamper & van den Bergh (1976)

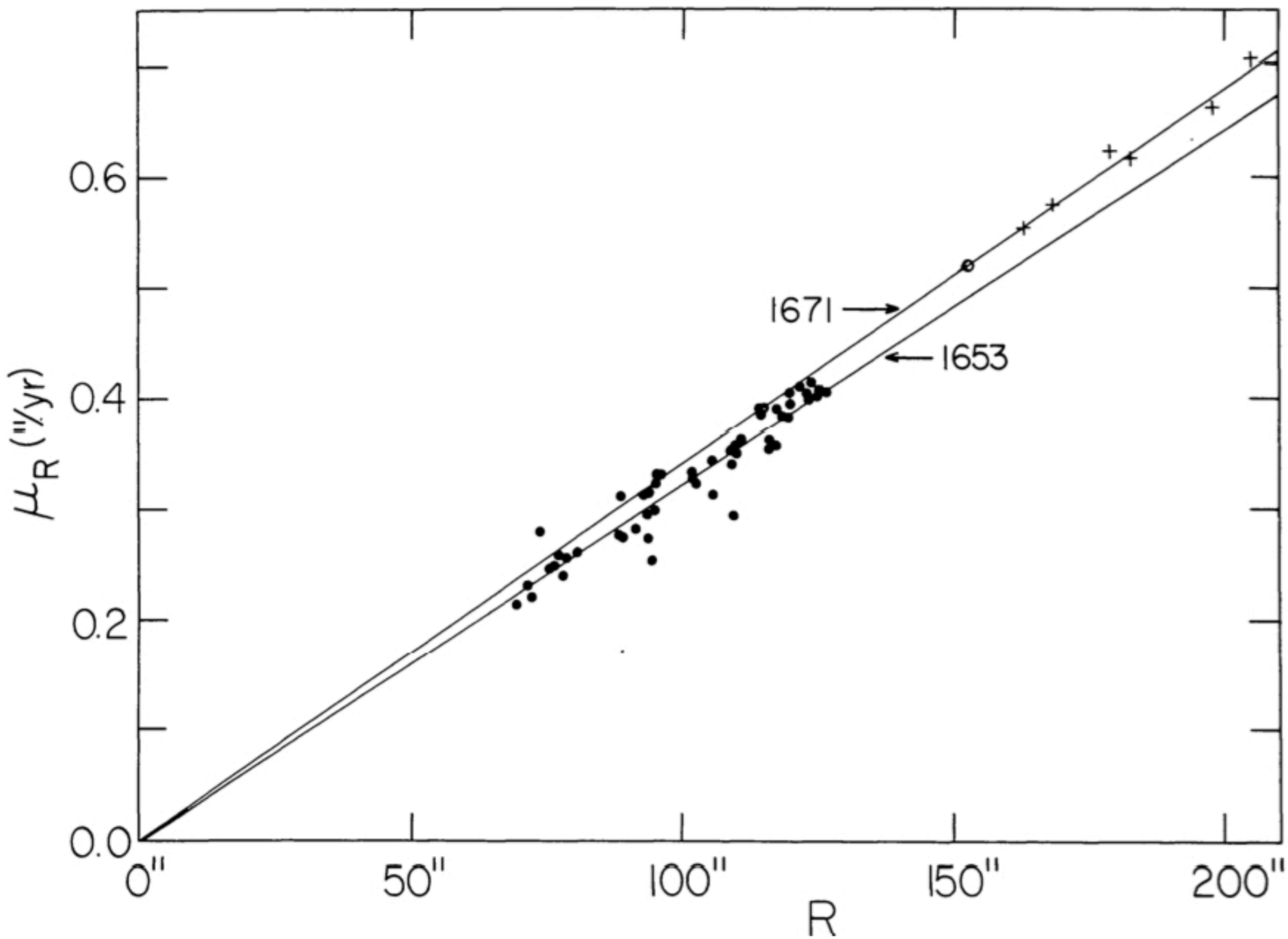

FIG. 11.—The figure shows that knots in the jet (+) and the isolated knot no. 91 (○) are expanding faster than objects in the main shell (●) of the supernova. Regression lines show expected relations for uniform expansion starting in 1653 and 1671, respectively.

Kamper & van den Bergh (1976)

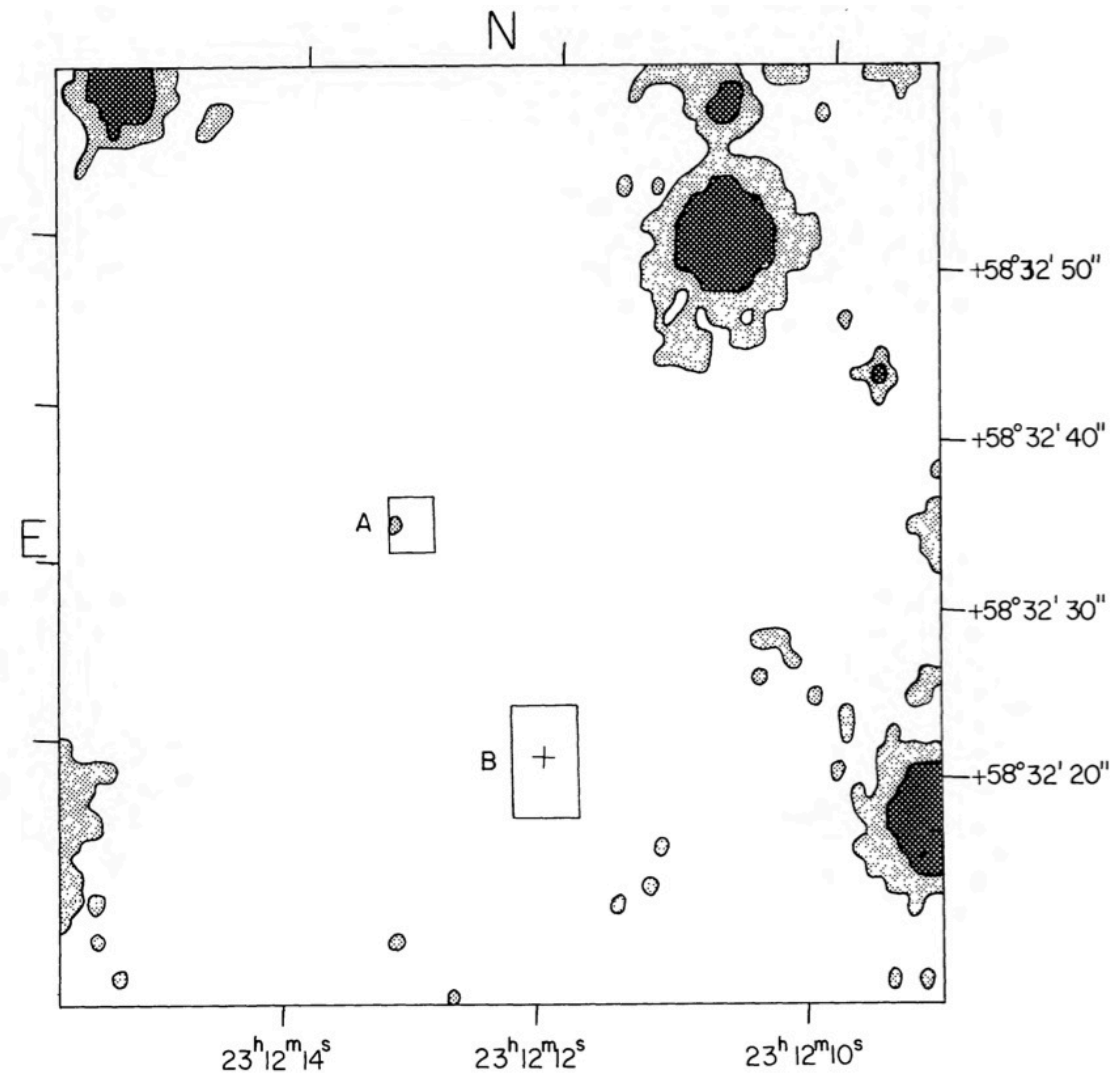

FIG. 15.—Contour map of region near center of expansion (*cross*) obtained by stacking scans of 10 red plates obtained with a PDS microdensitometer. Actual numerical data for the two small boxes shown in the figure are shown in Fig. 16. The star in the upper right-hand corner has red magnitude $r \approx 15$; that in the smallest box $r \approx 22$. The lowest contour represents a (smoothed) density that is 2 σ above the plate noise.

J. Astrophys. Astr. (1980) 1, 67–70

A Search for OB Stars in Supernova Remnants

Sidney van den Bergh *Dominion Astrophysical Observatory, Herzberg Institute of Astrophysics, Victoria, B.C., Canada*

Received 1980 April 30; accepted 1980 May 20

Abstract. A massive binary, in which the primary becomes a supernova, should leave a luminous secondary near the centre of its remnant. Contrary to expectation no statistically significant excess of OB stars is, however, found near the centres of optically visible galactic supernova remnants.

Sidney van den Bergh (1980)

2. Expected number of OB stars in SNR's

From data collected by Tammann (1974) it is seen that supernovae of type II outnumber those of type I by factors of 4/3 and 21/13 in Sb and Sc galaxies respectively. Since the Galaxy is generally considered to be of morphological type intermediate between types Sb and Sc $\sim$ 60 per cent of all galactic SNR's should have been produced by SN II. Of the 34 presently known optical SNR's in the Galaxy $\sim$20·4 should therefore have been formed by the explosion of the massive (*cf.* Maza and van den Bergh 1976) precursors of SN II. According to Garmany, Conti and Massey (1980) $\geqslant$37 per cent of all O stars are, on the basis of their radial velocities, certain or probable binaries. If it is assumed* that all primaries *and* secondaries become SN II then a fraction $\geqslant 37/(63 + 37 + 37) = 0{\cdot}27$ of all galactic SN II remnants were produced by primaries and should still contain OB secondaries. On the basis of this assumption $\geqslant$ 5·5 of the optically visible galactic SNR's should contain an OB star near their centres. The real number of OB stars in SNR's will be even greater than this because a large fraction of all OB stars are known to be members of wide physical double or multiple systems (Salukvadze 1979) such as the Orion Trapezium.

Sidney van den Bergh (1980)

is shown in Fig. 1. The observed distribution of R/R_m values within SNR's is seen to be indistinguishable from a uniform distribution. In particular only four stars are observed to have $R/R_m < 0{\cdot}20$, compared to 4·4 expected for a uniform distribution. In addition to Plaskett's star the following objects are found to have $R/R_m < 0{\cdot}20$: $+42°$ 1286 (B 0·5 V) in HB 9 and $+27°$ 828, $+27°$ 830 (OB$^-$) in S 147.

The Hamburg/Warner and Swasey identification charts show that spectral classification is still possible in the brightest part of the Cygnus Loop. This shows that the observed distribution of OB stars within SNR's is probably little affected by emission nebulosity.

No plausible explanation, other than the perversity of small-number statistics presents itself for the unexpected lack of OB stars at or near the centres of galactic supernova remnants.

Discovery of an OB runaway star inside SNR S147

B. Dinçel,[1★] R. Neuhäuser,[1] S. K. Yerli,[2] A. Ankay,[3] N. Tetzlaff,[1] G. Torres[4] and M. Mugrauer[1]

[1] *Astrophysikalisches Institut und Universitäts-Sternwarte Jena, D-07745 Jena, Germany*
[2] *Department of Physics, Orta Doğu Teknik Üniversitesi, 06531 Ankara, Turkey*
[3] *Department of Physics, Boğaziçi University, 34342 İstanbul, Turkey*
[4] *Harvard–Smithsonian Center for Astrophysics, 60 Garden St, Mail Stop 20, Cambridge, MA 02138, USA*

ABSTRACT

We present first results of a long-term study: Searching for OB-type runaway stars inside supernova remnants (SNRs). We identified spectral types and measured radial velocities by optical spectroscopic observations and we found an early type runaway star inside SNR S147. HD 37424 is a B0.5V-type star with a peculiar velocity of $74 \pm 8\,\mathrm{km\,s^{-1}}$. Tracing back the past trajectories via Monte Carlo simulations, we found that HD 37424 was located at the same position as the central compact object, PSR J0538+2817, 30 ± 4 kyr ago. This position is only ∼4 arcmin away from the geometrical centre of the SNR. So, we suggest that HD 37424 was the pre-supernova binary companion to the progenitor of the pulsar and the SNR. We found a distance of 1333^{+103}_{-112} pc to the SNR. The zero-age main sequence progenitor mass should be greater than $13\,\mathrm{M}_\odot$. The age is 30 ± 4 kyr and the total visual absorption towards the centre is 1.28 ± 0.06 mag. For different progenitor masses, we calculated the pre-supernova binary parameters. The Roche lobe radii suggest that it was an interacting binary in the late stages of the progenitor.

MNRAS, 448, p. 3196 (2015)

Dincel et al. (2015)

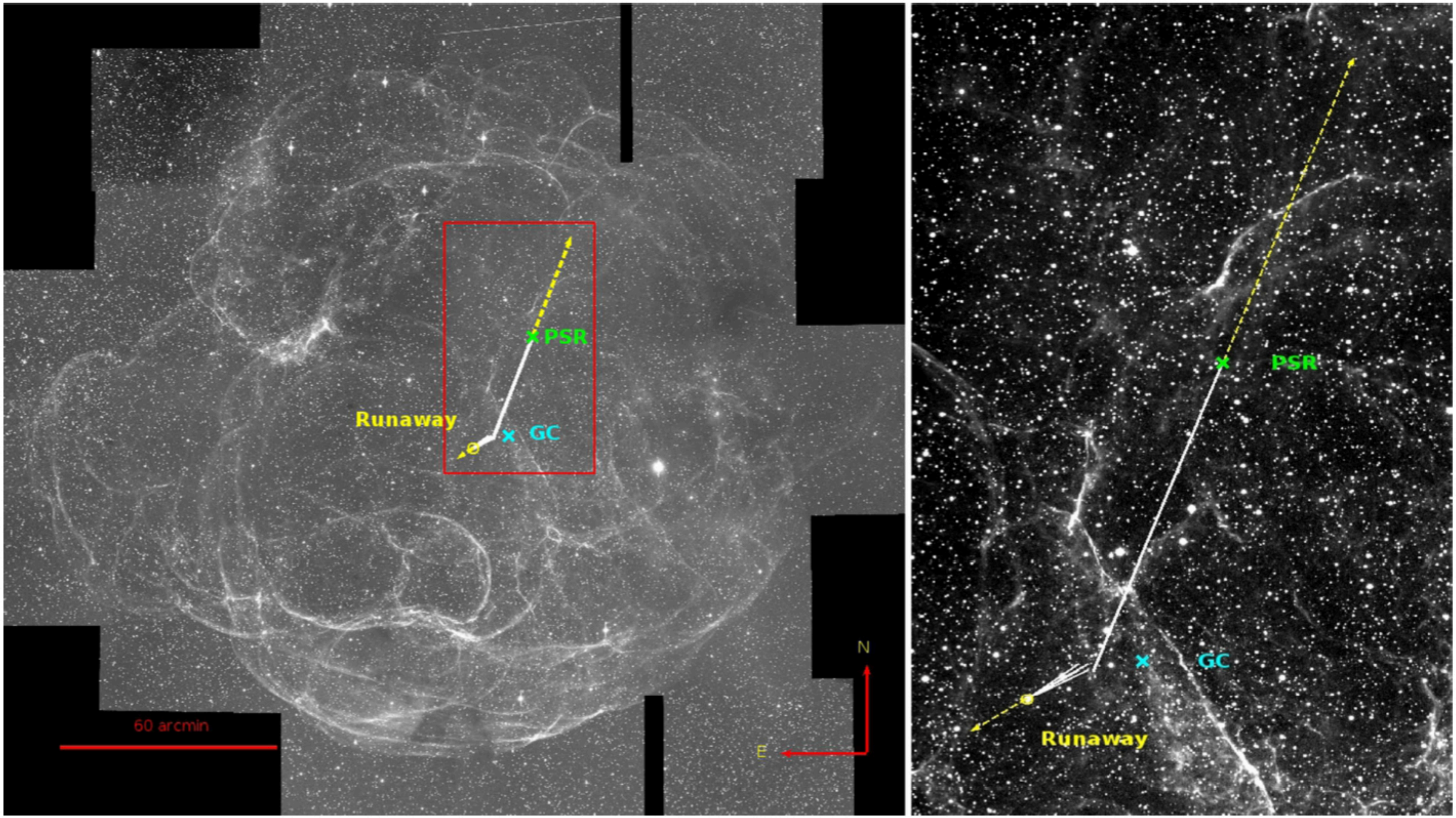

Figure 1. The 4°.8 × 4°.1 Hα image of SNR S147 taken at the University Observatory Jena. The green cross represents the pulsar, the cyan cross shows the GC of the SNR and the yellow circle is HD 37424. The yellow vectors show the pm of the objects. The red box is the zoom-in area shown in the right-hand panel. The white arrows are the tracing back cones of the pm for 29 300 yr. The angle between the pm vectors is 139°–148° In 2D calculations, both objects come towards each other as close as 0.126 pc which means that they have a common origin: binary SN disruption.

SNRs and ^{44}Ti

- Exclusively produced in SN explosion

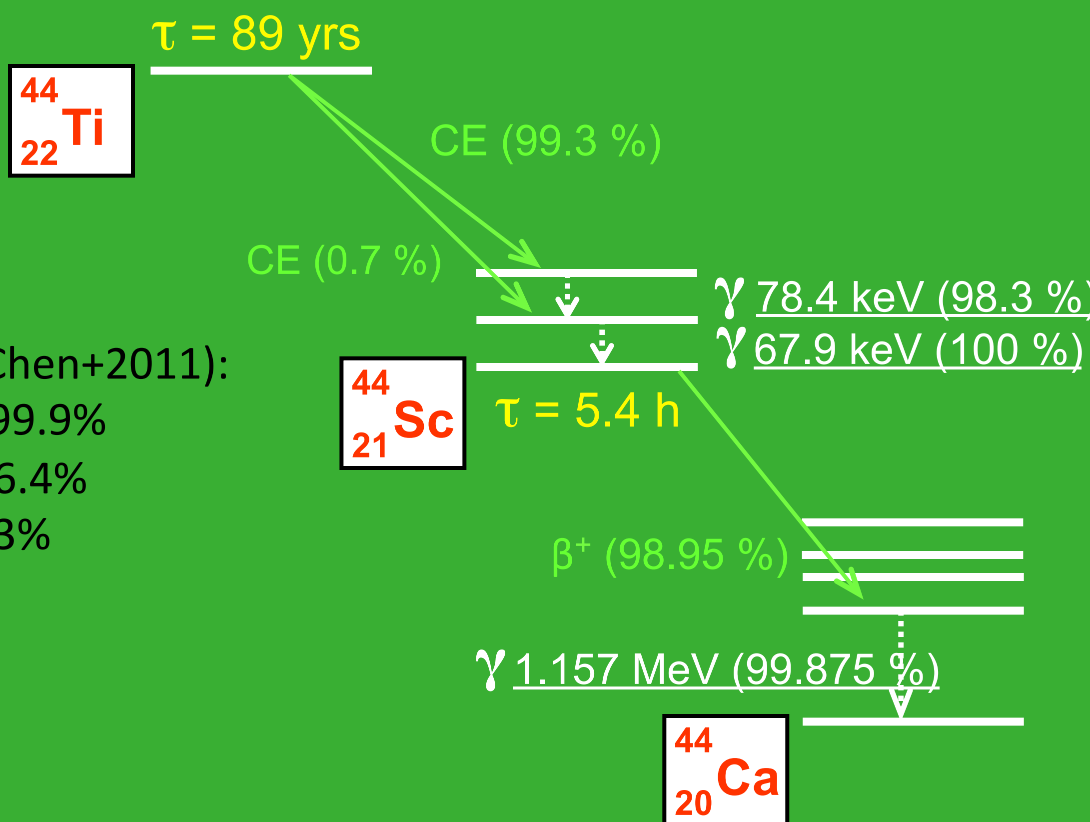

Branching (Chen+2011):
1.157 MeV-99.9%
78.32 keV-96.4%
67.87 keV-93%

^{44}Ti γ-ray lines ⇔ young SNRs (age < 1000 yrs)

Asymmetric explosion required !?

Optical spectroscopy → asymmetric explosion (jets??)
$V_{exp} \geq V_{transverse} \approx$ 6500—14500 km/s
(Fesen et al. '06; Hammel and Fesen '08);
$V_{transverse} \approx$ 12700—15600 km/s
(Fesen+Milislavljevic '15)

From gamma-spectroscopy we get:

From ^{44}Ti line FWHM, for ^{44}Ti rich ejecta velocity was derived:
v_D= 5350±1610 km/s,
as measured by NuSTAR at 68 keV (Grefenstette+2014);
v_D= 2200±400 km/s,
as measured by SPI for 1.157 MeV (Siegert+2015);
v_D= 4300±1600 km/s,
measured by SPI at 78 keV line (Siegert+2015);
v_D= 7200±2900 km/s,
measured by COMPTEL at 1.157 MeV (Iyudin+97)!

CasA ejecta extent (Fesen+Milislavljevich’16)

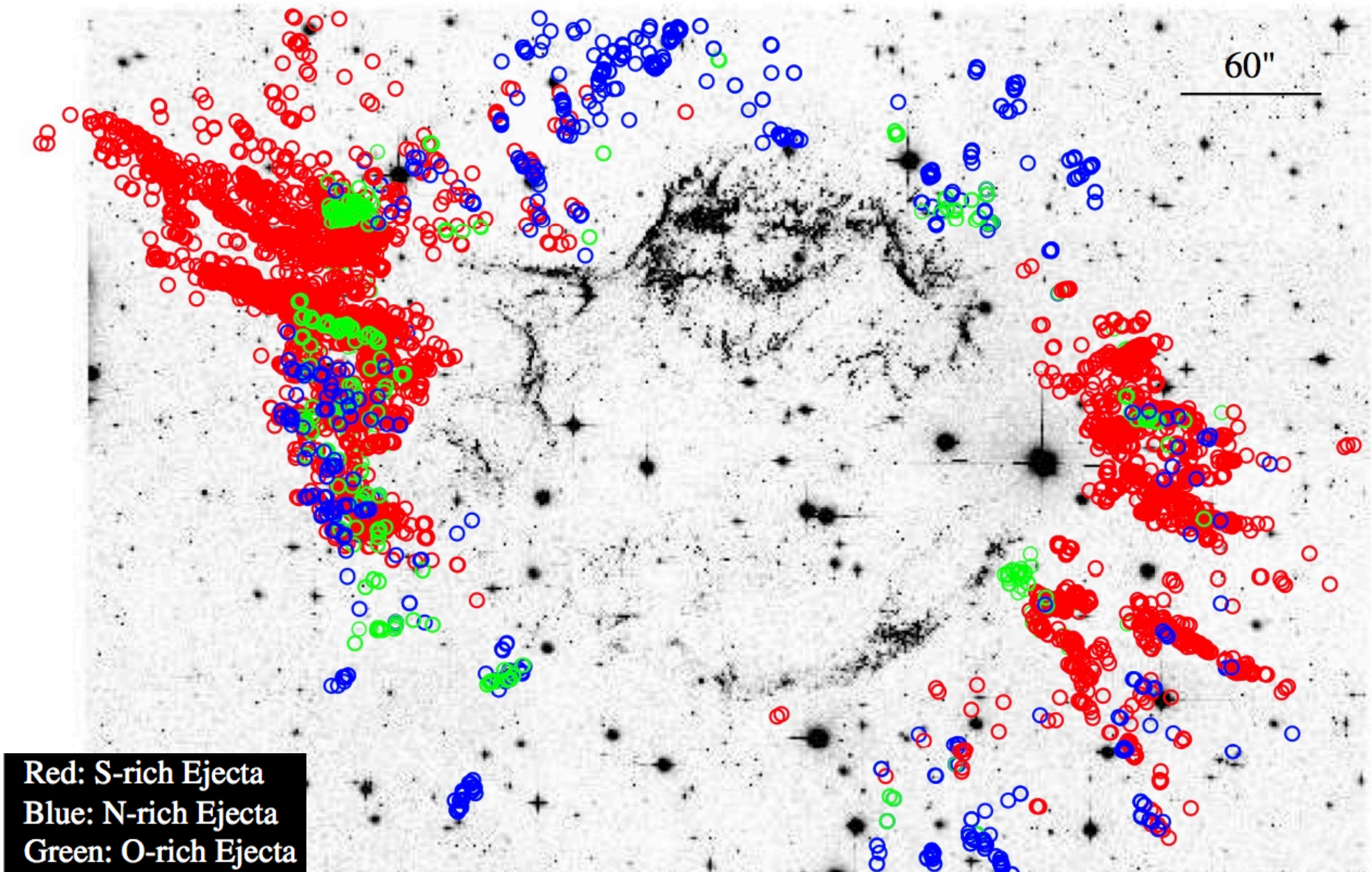

Fesen+Milislavljevich’16

We have identified ∼3400 S-rich knots from the WFC3 [S II] + [S III] images. Using the above knot mass estimate, this means a total mass of $\sim 0.03\ M_\odot$ for high-velocity S-rich ejecta. Although much of the NE jet’s emission arises from a few dozen larger knots with angular diameters of $0\farcs2$ to $0\farcs4$ and hence are the most massive, they are not numerous enough to significantly change this mass estimate.

However, this mass estimate of outlying ejecta is likely a lower limit since it pertains only to dense clumps. Extended diffuse material in both jets cannot be ruled out, plus as noted above there may be hundreds more knots undetected in our survey in the SW jet along the western limb due to significant extinction there. This along with possible emission filling factors greater than 0.5 means that the total jet/counterjet mass could be $\sim 0.1\ M_\odot$.

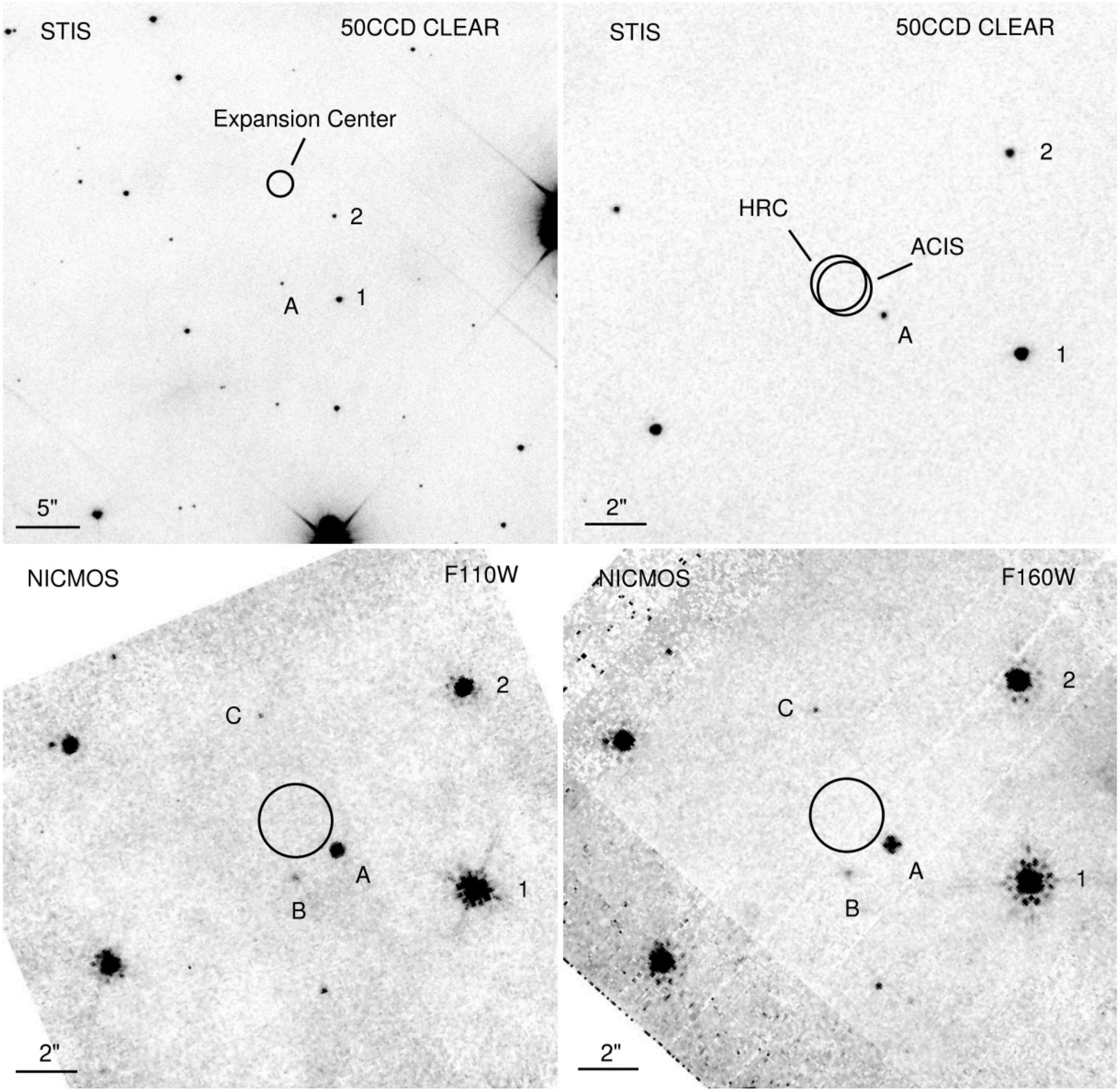

ApJ, 636 (2006)

Search for CCS
HST *& Chandra*

Cas A CCS properties

TABLE 5

Observed Optical and Near IR Magnitudes for Radio-Quiet Neutron Stars

Object	SNR	R (mag)	J (mag)	H (mag)	K_s (mag)	References
CCOs						
Cas A XPS	G111.7−2.1 (Cas A)	≥27.8	≥26.2[a]	≥24.6[a]	≥21.2	1–4
CXOU J0852−4617	G266.2−1.2 (Vela Junior)	≥22.0	...	...	...	5, 6
1WGA J1713−3949	G347.3−0.5	...	...	...	...	7
RX J0822−4300	G260.4−3.4 (Pup A)	≥24.8	...	...	...	8, 9
1E 1207−5209[b]	G296.5+10.0 (PKS 1209−51/52)	≥26.6	≥23.5	≥22.4	≥22.0	10
RX J1853+0040	G33.6+0.1 (Kes 79)	≥24.9	...	...	...	11, 12
AXPs						
XTE J1810−197	...	≥21.5	≥23.0	22.0–22.7[c]	20.8–21.4[c]	13–16
1E 1048−5937	...	≥24.8	21.7–23.4[c]	20.8–(≥21.5)[c]	19.4–21.3[c]	17–20
1E 1841−045	G27.4+0.0 (Kes 73)	≥23.0	≥22.1	≥20.7	≥19.9	21–23
CXOU J0100−7211[d]	...	24.2[e]	...	...	...	24–27
1RXS J1708−4009[d]	...	≥26.5	20.9	18.6; 18.85[f]	18.3; 17.5[f]	28
4U 0142+614	...	24.9	...	...	19.7–20.2[c]	29, 30
1E 2259+586	G109.1−1.0 (CTB 109)	≥26.4	≥23.8	...	20.4–21.7[c]	31–34

[a] $m_{\rm F110W} \approx J$; $m_{\rm F160W} \approx H$.

Fig. 2.—*HST* images of the Cas A central region near the XPS. *Top left:* 2001 STIS image of the remnant's central region with the Thorstensen et al. (2001) expansion center indicated ($\alpha = 23^{\rm h}23^{\rm m}27\overset{\rm s}{.}77 \pm 0\overset{\rm s}{.}05$, $\delta = 58°48'49\overset{''}{.}4 \pm 0\overset{''}{.}4$). *Top right:* Enlargement of the STIS image with the 95% confidence level circles marked for *Chandra* ACIS-S (radius $= 0\overset{''}{.}9$) and HRC-S (radius $= 0\overset{''}{.}9$) centered on the respective mean positions for each data set as listed in Table 2. Star A lies closest to the nominal XPS position but is likely a foreground late-type star (Kaplan et al. 2001). Lower panels show NICMOS J- and H-band images of the Cas A central region with 99% confidence level circles (radius $= 1\overset{''}{.}2$) shown centered on our adopted position for the XPS ($\alpha = 23^{\rm h}23^{\rm m}27\overset{\rm s}{.}943$, $\delta = 58°48'42\overset{''}{.}51$; see text and Table 2). While the NICMOS H-band image revealed a few faint, additional sources (B and C) near the XPS, no source is detected within the *Chandra* error circle.

Cas A
CCS

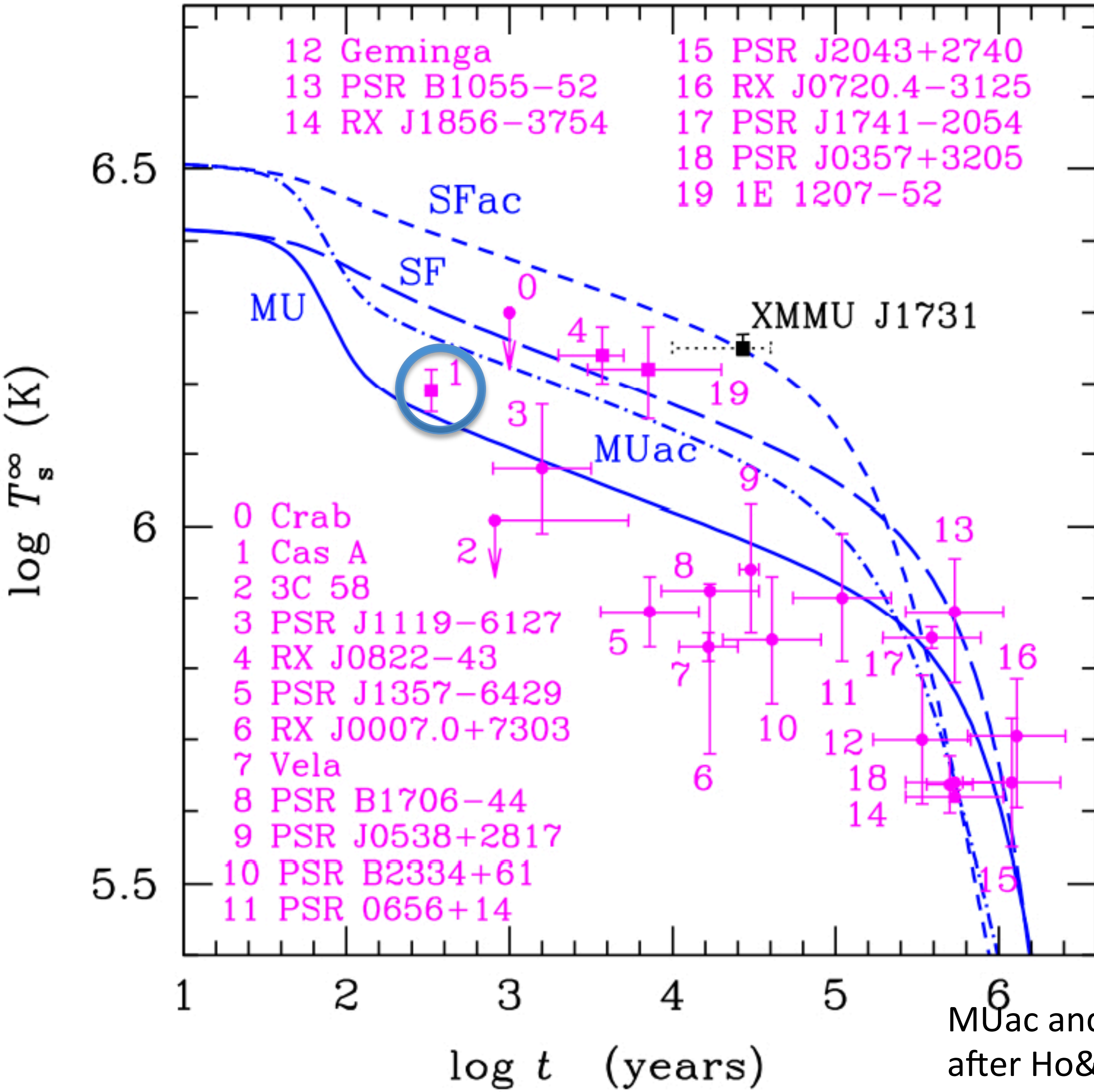

Klochkov et al. (2015)

-- Cas A

MUac and SFac are suggested after Ho&Heinke (2009) paper!

CCS cooling curves

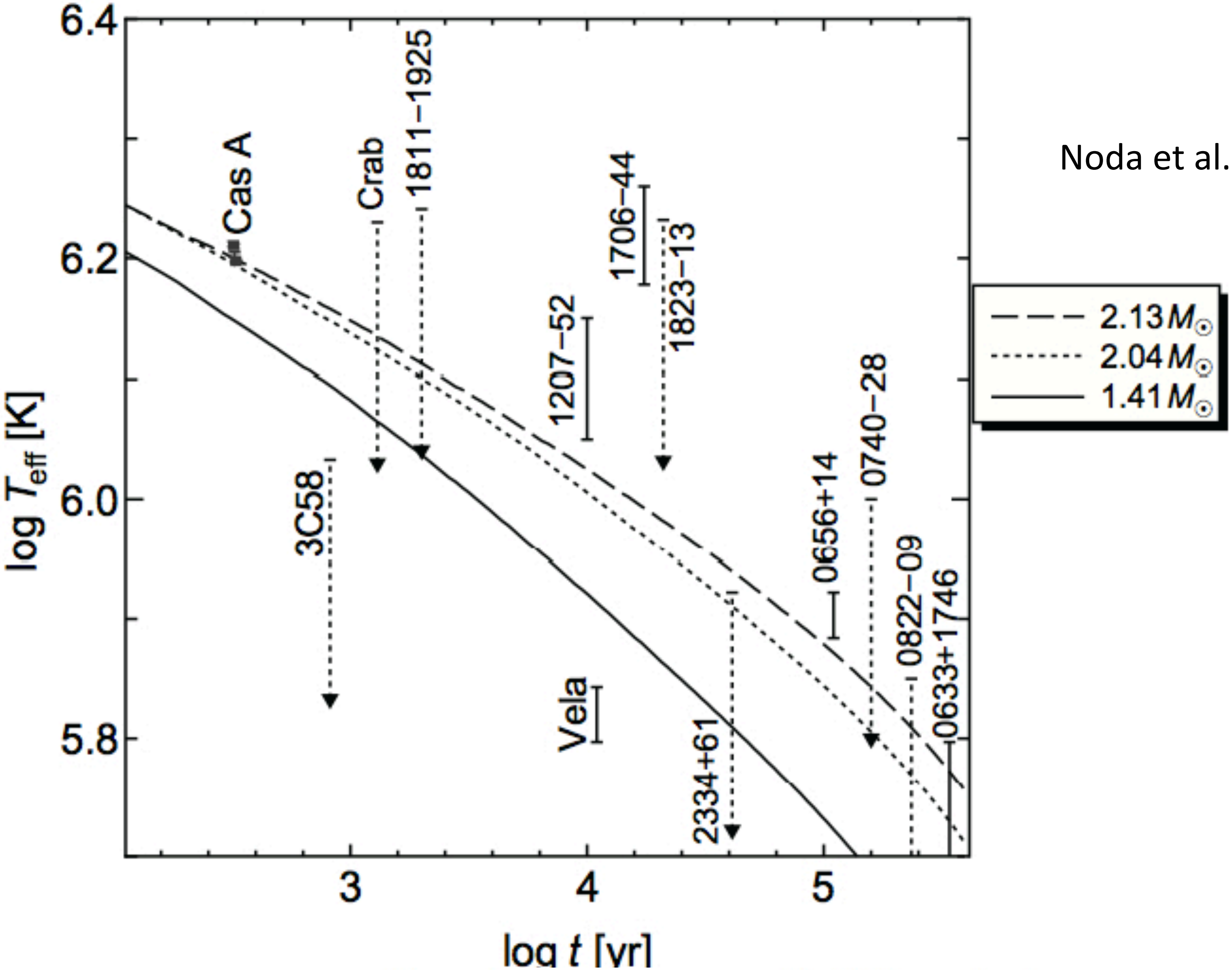

Noda et al. (2015)

Figure 1: Cooling curves with CSC quark phases.

Cas A 3D structure

Spitzer data,
Figure from
DeLaney+2010

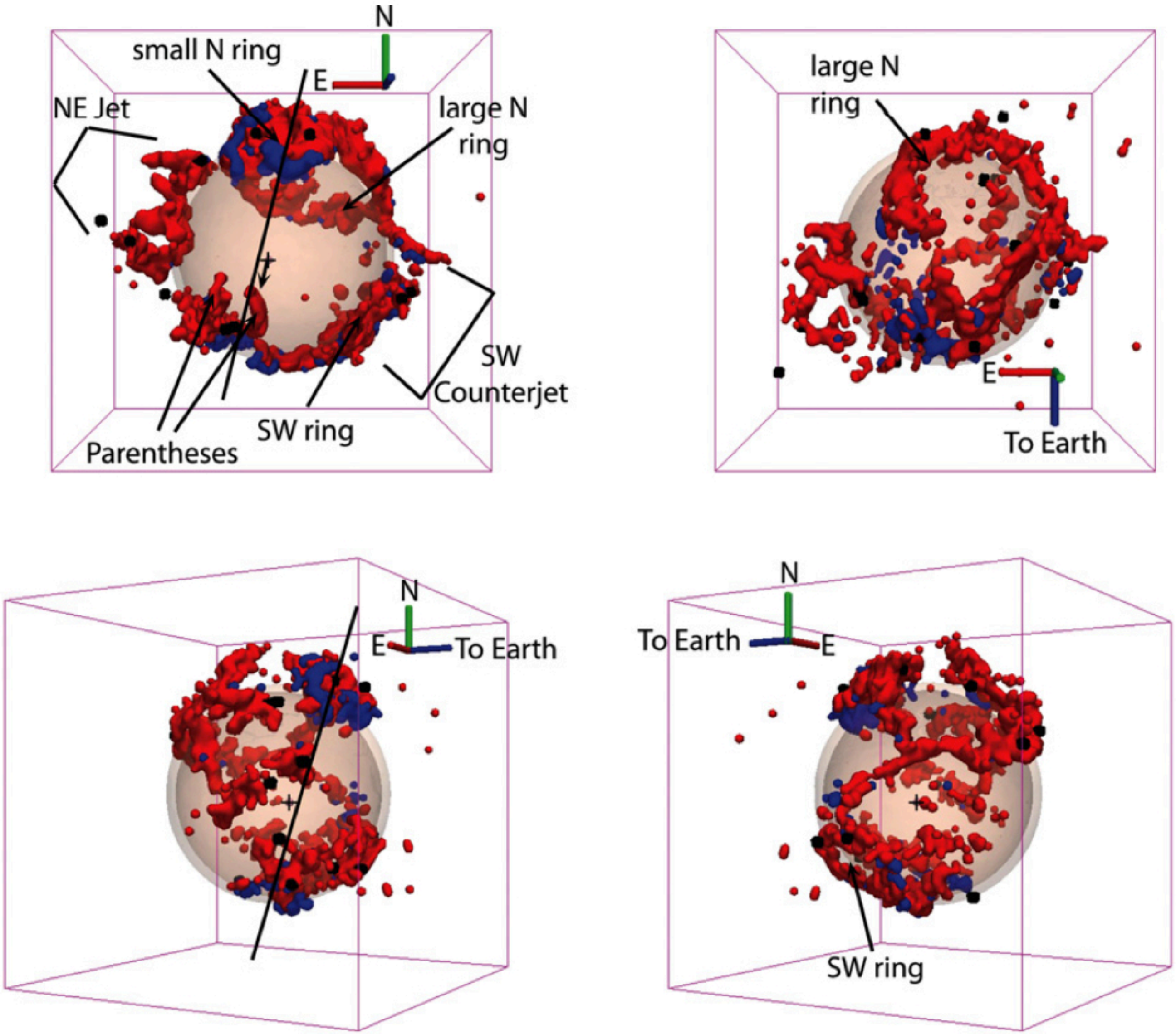

Figure 13. Three-dimensional projections of the infrared [Ar II] emission (red), X-ray Si XIII emission (black), the fiducial reverse shock (sphere), and the CCO (cross). Locations where the [Ne II]/[Ar II] ratio are high are indicated in blue. The lines in the top left and bottom left panels identify an apparent symmetry axis for the Ne-rich regions. The inferred CCO proper motion direction is indicated in the top left panel. Major structures discussed in Section 4.3 are indicated. The individual views are: top left, from Earth; top right, from the north; bottom left, 60° rotation to the east; bottom right, 120° rotation to the west. These same four projections will be used for all subsequent three-dimensional figures.

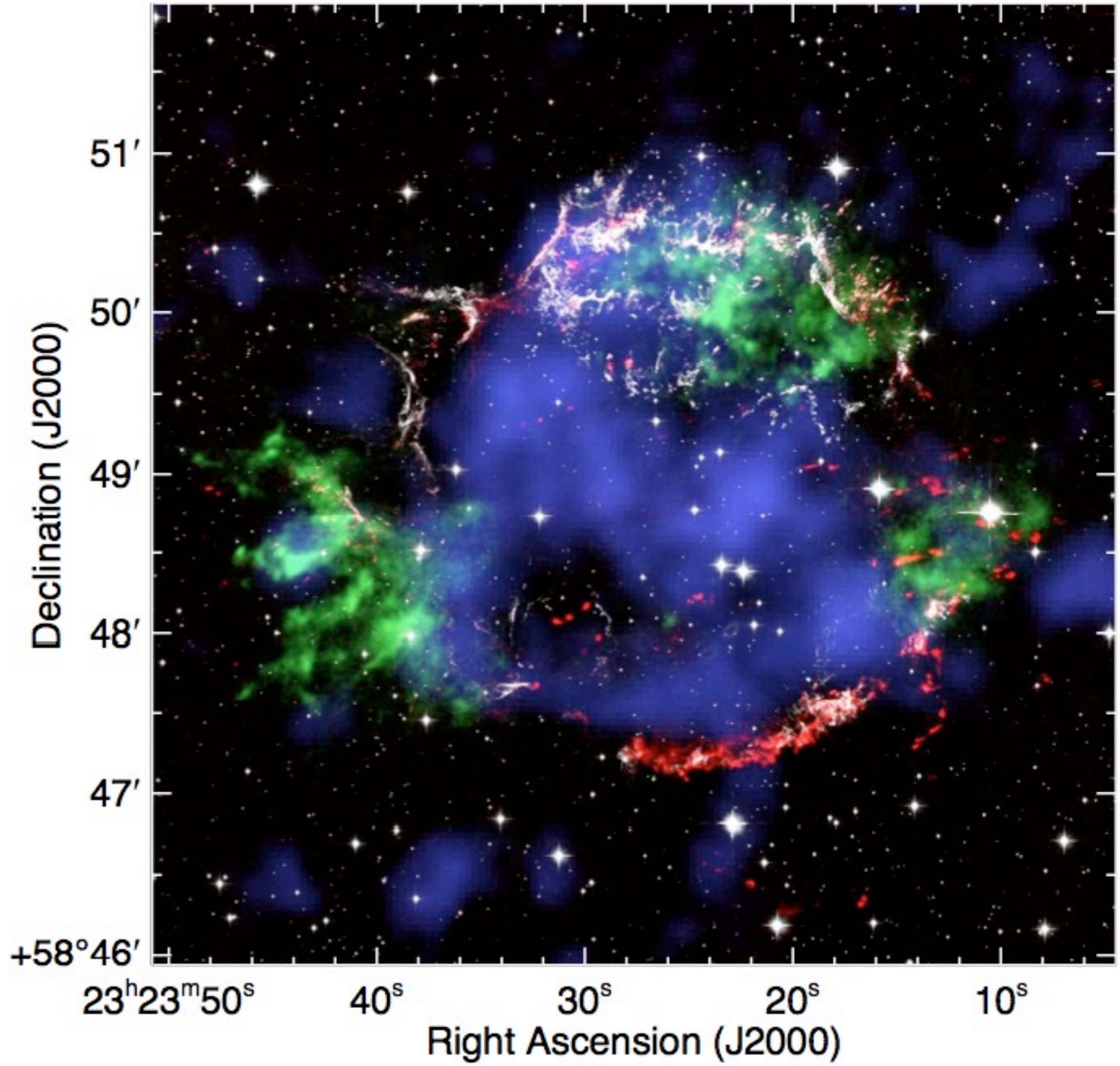

A four-color composite image of Cas A with the [Fe II] 1.644 μm narrow-band image from Fig. 1 of Park et al. (2016) in red, The *Chandra* Fe K-shell (6.52-6.94 keV) image in green (Hwang et al. 2004), the NuSTAR hard X-ray ^{44}Ti (67.9 and 78.4 keV) image in blue (Grefenstette et al. 2014), and the HST ACS/WFC F850LP image in white (Fesen et al. 2006).

Surface brightness map in [Fe II] line at 17.94 μm

Smith et al. (2009)

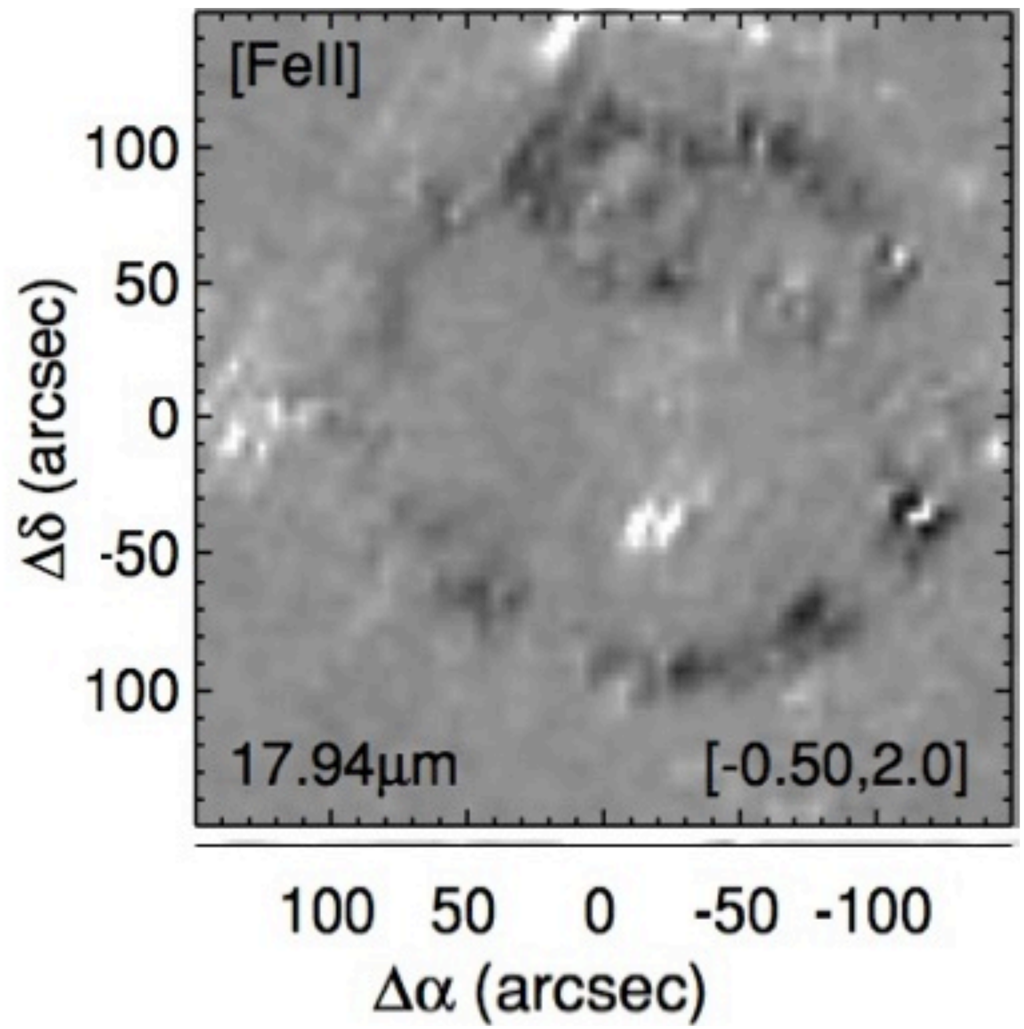

Lee et al. (2017)

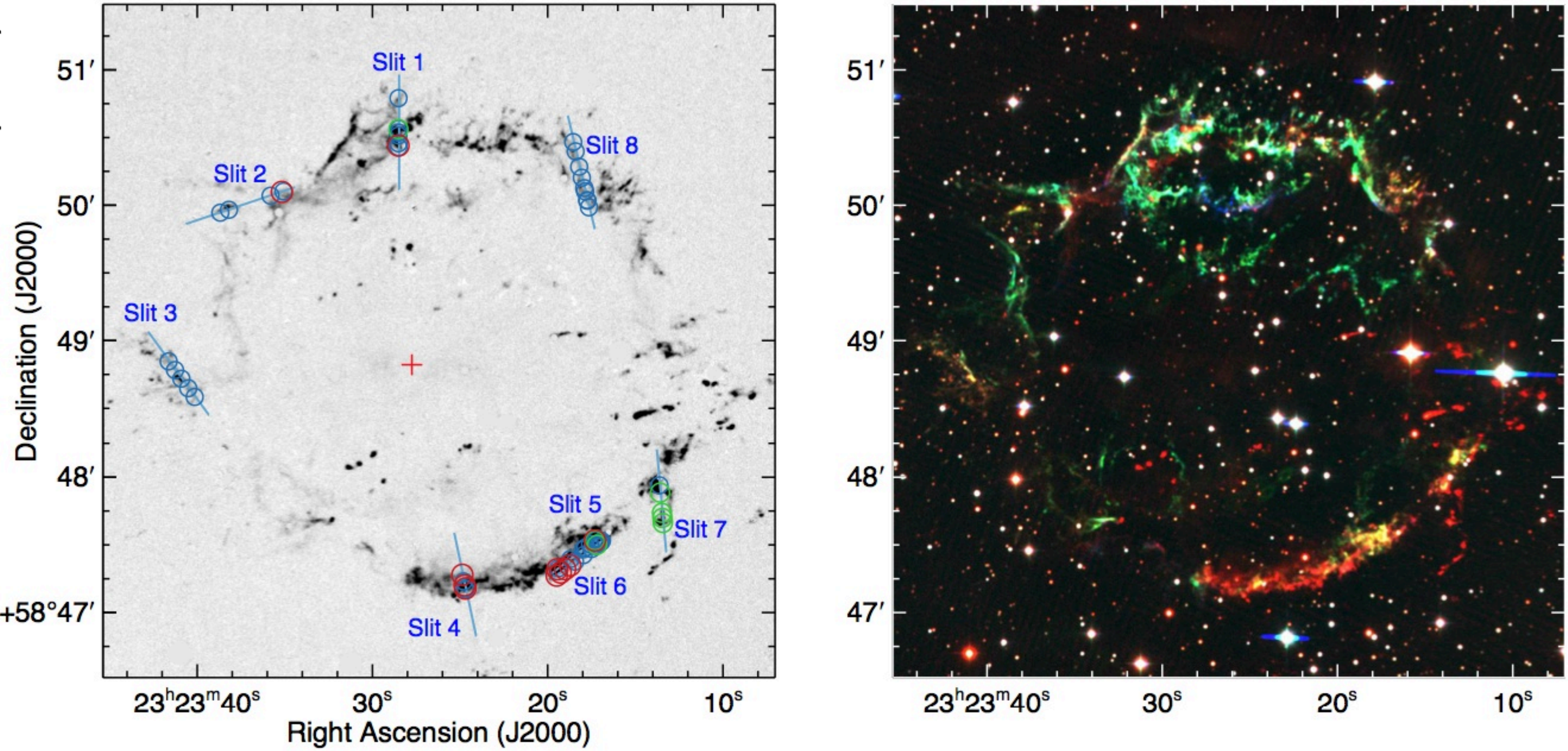

Fig. 10.— (Left) Locations of 63 knots in Table 2. (See Figure 3 for the knot numbers in each slit.) The He-rich, S-rich, and Fe-rich knots are marked in green, blue, and red, respectively. The background is the continuum-subtracted [Fe II] 1.644 μm narrow-band image in Figure 1. (Right) A three-color composite image of Cas A with an [Fe II] 1.644 μm narrow-band image in red, and *HST* ACS/WFC F850LP and F775W images in green and blue. The *HST* images are dominated by [S III] 9069, 9531 Å and [S II] 1.03 μm multiplets (F850LP) and [O II] 7319, 7330 Å lines (F775W), respectively (Fesen et al. 2006; Hammell & Fesen 2008). The [Fe II] 1.644 μm image was observed in 2005 August. The *HST* ACS/WFC images are from the Hubble Legacy Archive (https://hla.stsci.edu) and

NIR observations: Lee et al. ‘15, ’17;

We performed NIR spectroscopic observations of Cas A in which we obtained the spectral and kinematical properties of 63 [Fe II]-line-emitting knots spread over the main ejecta shell. All of the knots show strong [Fe II] 1.26 and 1.64 μm lines, the ratio of which provides a direct measure of the extinction. From an analysis of the extinction toward individual knots, we showed that the NIR extinction is due in part to SN dust within the remnant. We explored the nature of the SN dust responsible for the NIR extinction by analyzing its thermal infrared emission.

NIR spectroscopy at 0.94-2.46 **μ**m performed with the use of TripleSpec mounted on the Palomar 5 m Hale telescope. TripleSpec is a cross-dispersed NIR spectrograph with Resolving power of R~2700 (Wilson et al. 2004; Herter et al. 2008). The spectrograph Uses Rockwell Scientific Hawaii-II array with two arrays of 2048x1024 size combined.

Conclusion from NIR -1

1. We found that [Fe II] emission from redshifted SN ejecta is in general more heavily obscured than that from blueshifted SN ejecta (Figure 2). We interpret the correlation as evidence for newly formed SN dust within the remnant. The amount of excess extinction varies considerably from one sight line to another, which suggests a highly non-uniform distribution of SN dust.

Excerpt from Lee et al. (2017)

Conclusion from NIR - 2

When the cool dust is pure Fe grains, we can make a crude estimation of the dust formation efficiency from our observation. The required Fe dust mass density of (2–5) $\times 10^{-4}$ g cm^{-2} corresponds to an Fe nucleus column density of (2–5) $\times 10^{18}$ cm^{-2}. For comparison, the characteristic size of [Fe II]-line-emitting clumps is 5″ or 0.08 pc at 3.4 kpc, and their average electron density is 2×10^4 cm^{-3} (Koo et al. 2013). For pure Fe ejecta clumps, because Fe is mostly in Fe^+, it means that the number density of Fe atoms is 2×10^4 cm^{-3}, and the characteristic Fe column density in the gas phase of Fe ejecta clumps is $N_{\rm Fe} \sim 5 \times 10^{21}$ cm^{-2}. Therefore, if there are $n_{\rm clump}$ such clumps along the sight line where $E(J - H) \approx 0.23$ in Slit 4, we obtain a dust-to-gas ratio of $(0.4-1) \times 10^{-3}\, n_{\rm clump}^{-1}$.

Excerpt from Lee et al. (2017)

Sketch of the basic picture of CSM interacting SNe (Smith et al. 2008)

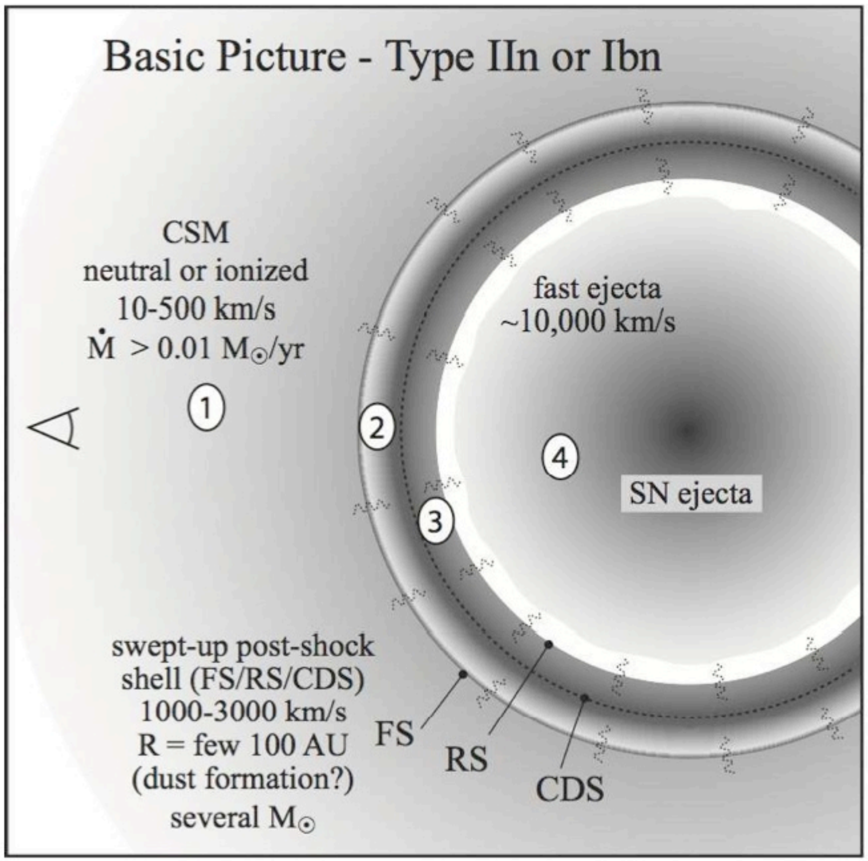

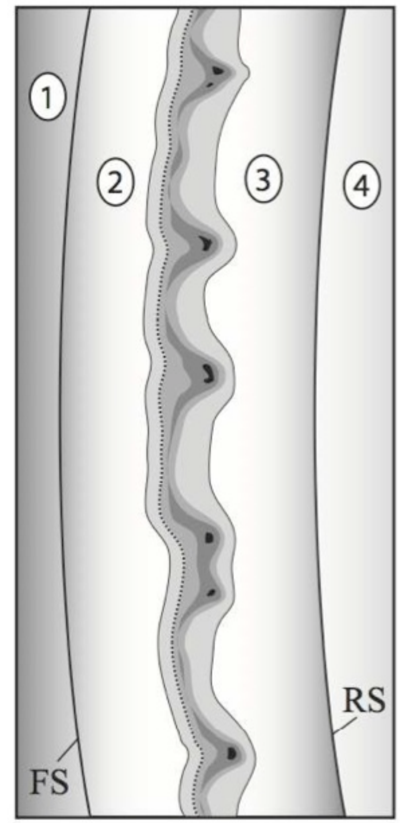

cold dense shell

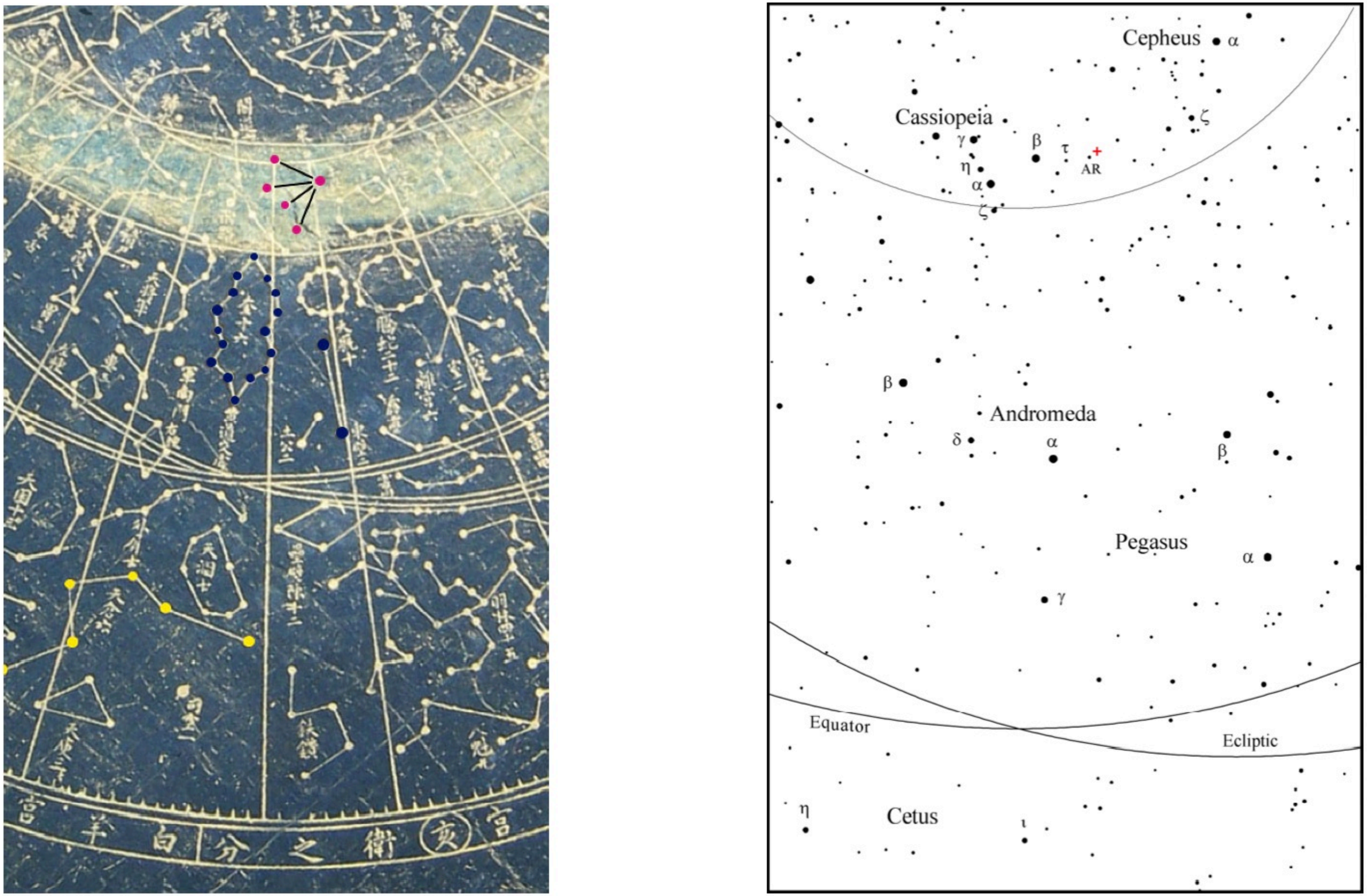

Figure 3. *Left:* A part of *Cheonsang Yeolcha Bunyajido* 天象列次分野之圖, the old Korean constellation map of *Joseon* dynasty made in 1395, showing the constellations *Wangyang* 王良, pink dots), *Byeok* (壁, right two dark blue points), *Gyu* (奎, left 16 dark blue points), and *Cheonchang* (天倉, yellow dots at bottom left). The right most star of *Wangyang* is β Cas, and the right-most star of *Cheonchang* is ι Cet. The epoch of this map is around 1st century A.D (Park 1998). *Right:* Position of the stars near Cassiopeia and Cetus brighter than 5.5 in visual magnitude in 1592. The expansion center of Cas A is marked with a small cross near AR Cassiopeia. The angular distance between β Cas and the expansion center is 5.9 degrees.

Park et al. (2016)

Cas A progenitor activity

For the Cas A SNR it is important to take seriously the 1592-1593 AD observations by Korean astronomers of the so-called “Guest-Star” near position of Cas A (Park et al. 2016). If this 1592-1593 AD “Guest-Star” was some type ejection activity of Cas A progenitor, similar to the 1843 outburst of eta-Carina (Smith et al. 2006), or to other “impostors”, then it is quite possible that notable mass of the Cas A pre-supernova was ejected during this event, producing already some amount of dust during ~80 years of pre-supernova CSM evolution before final explosion of Cas A around 1671 AD (Thorstensen et al. 2001; Soria et al. 2013). This dust was later making a “Veil” for the final Cas A SN explosion.

On the possible binary origin of SNe Cas A: it is very similar to SN1993J!

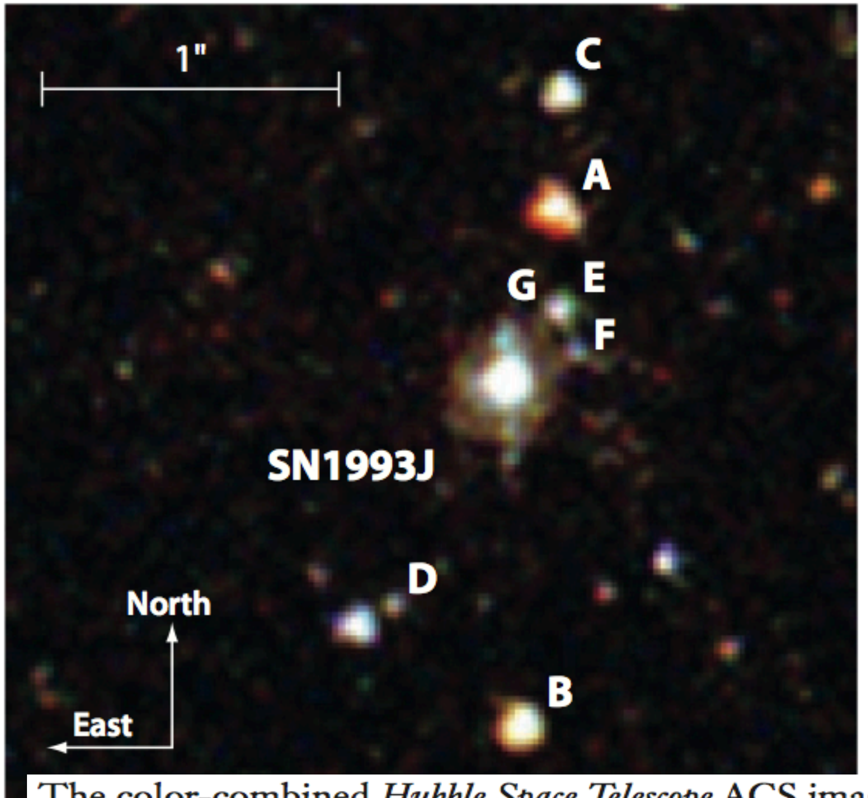

From Maund et al. (2004)

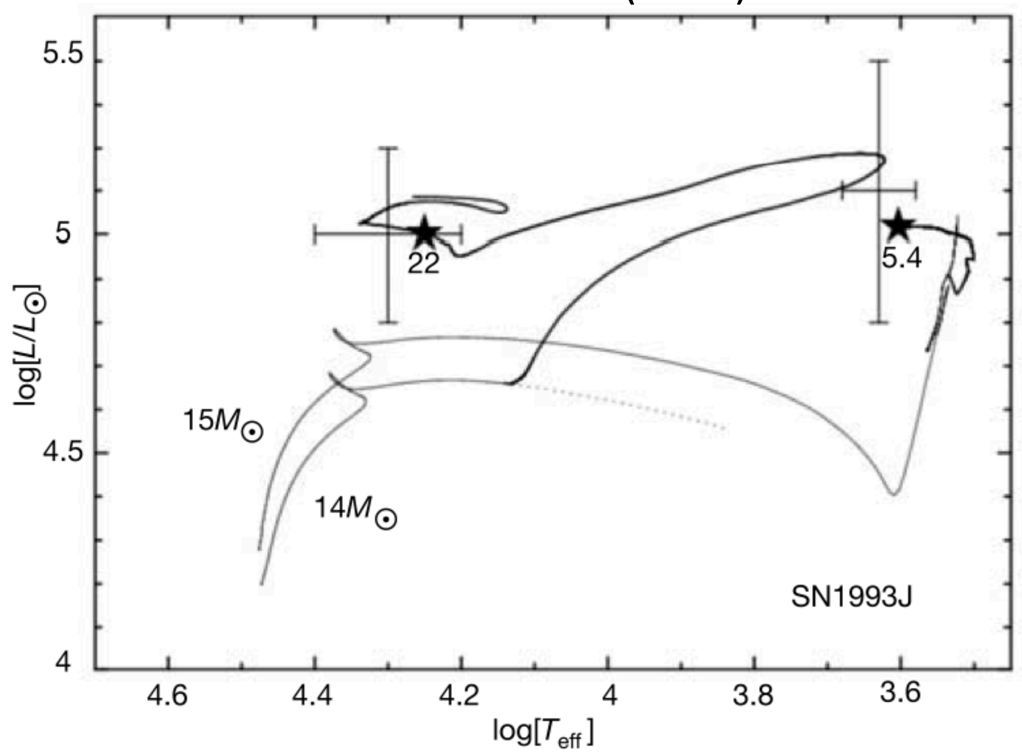

The color-combined *Hubble Space Telescope* ACS image of SN1993J at 10 years after explosion from Maund et al. (2004). The progenitor of SN1993J was a bright source in the *U* and *B* bands that could either have been due to a surrounding OB-association or binary companion in the lower resolution ground-based pre-explosion images of Aldering et al. (1994). The faint blue stars E, F, and G did contribute to the *UB*-band excess in the pre-explosion images but they cannot account for all of the progenitor's flux. A spectrum of the SN1993J source shows HI absorption lines due to a B-type supergiant star coincident with the SN1993J remnant, and this is likely the companion to the K-type supergiant that exploded and the main source of *UB*-band flux in the pre-explosion images (Maund et al. 2004). The exposures were taken through two near-UV filters (250 W, 2100 s and 330 W, 1200 s) shown in purple and blue, a blue filter (435 W, 1000 s) shown in green, and a green filter (555 W, 1120 s) shown in red [Image credit: European Space Agency. Adapted and reprinted by permission from Macmillan Publishers Ltd: Nature (Maund et al. 2004),

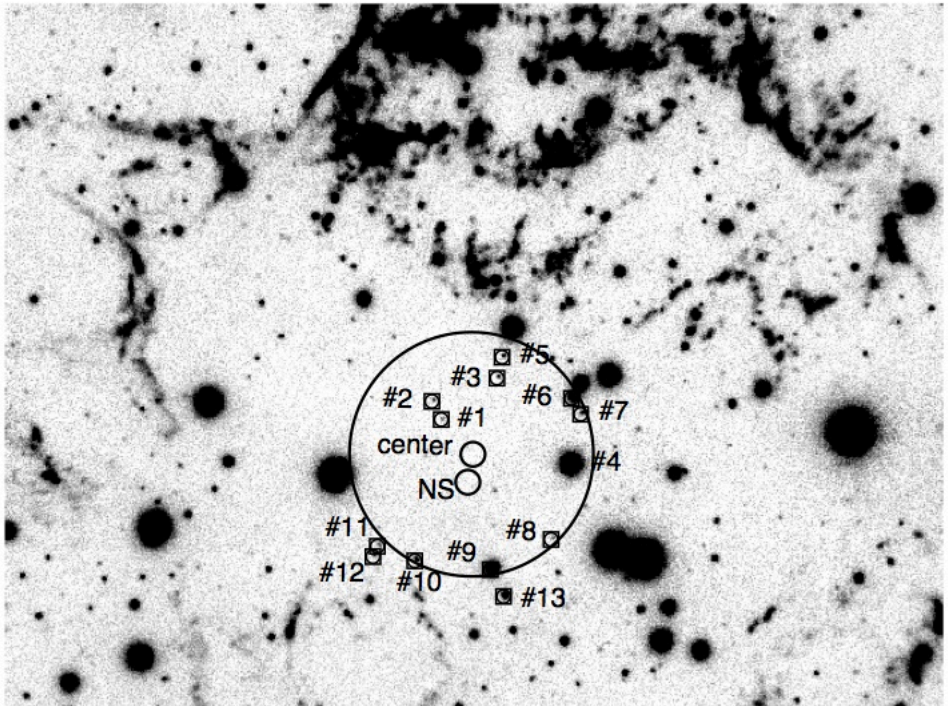

Kochanek (arXiv: 1701.03109) consider Cas A origin in a binary system unlikely

"Apart of absence of a star with a high velocity of proper motion near Cas A center, also a brightness limit put constrain on the possible binary presence near Cas A!"

Also a dust mass of Cas A makes its origin in a binary system questionable!

Figure 4. Coadded grizy PS1 image of Cas A. The position of the geometric center of the remnant ("center") and the neutron star are indicated by $3''.0$ radius circles. The larger circle shows the region within $30''.0$ of the center. The 13 PS1 stars lying within $30''.0$ of either the geometric center or the neutron star are marked and labeled in order of their distance from the center. None of the stars have proper motion measurements in NOMAD. Stars #4, #9 and #13 have proper motions in HSOY but the shift in position to the time of the SN is too small to display. At a distance of 3.4 kpc, a star will have moved $2''.1(v/100\ \mathrm{km/s})$ since the SN, so the $30''.0$ search radius corresponds to a velocity of roughly 1500 km/s

Dust in SN 1993J and Cas A (Bevan+2017)

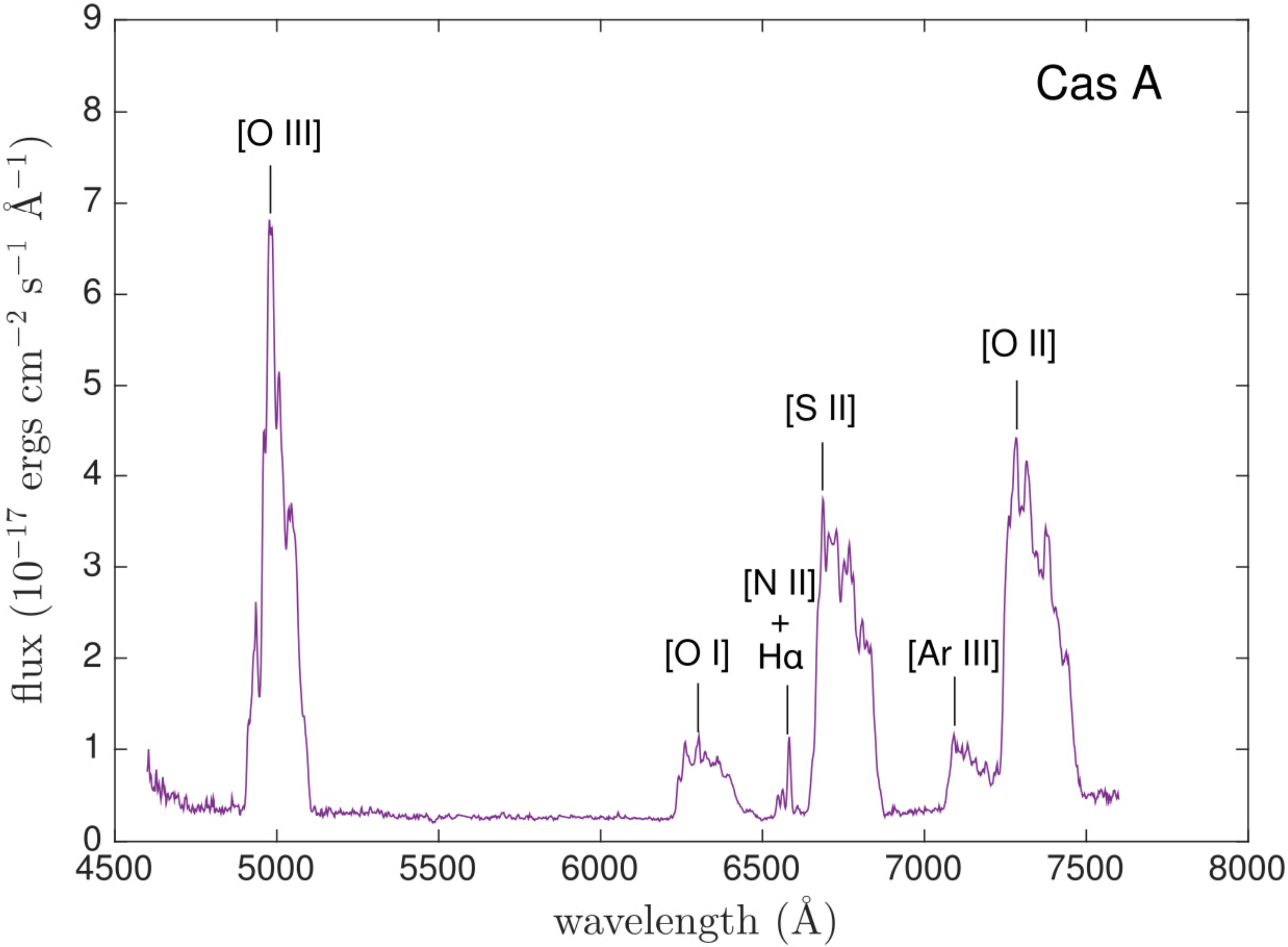

Dust in SN 1987A

Dust mass was derived based on the use of the DAMOCLE code described in Bevan&Barlow (2016) and on the line assymmetry measurements and profile fits for [OIII], [OII] and [OI].

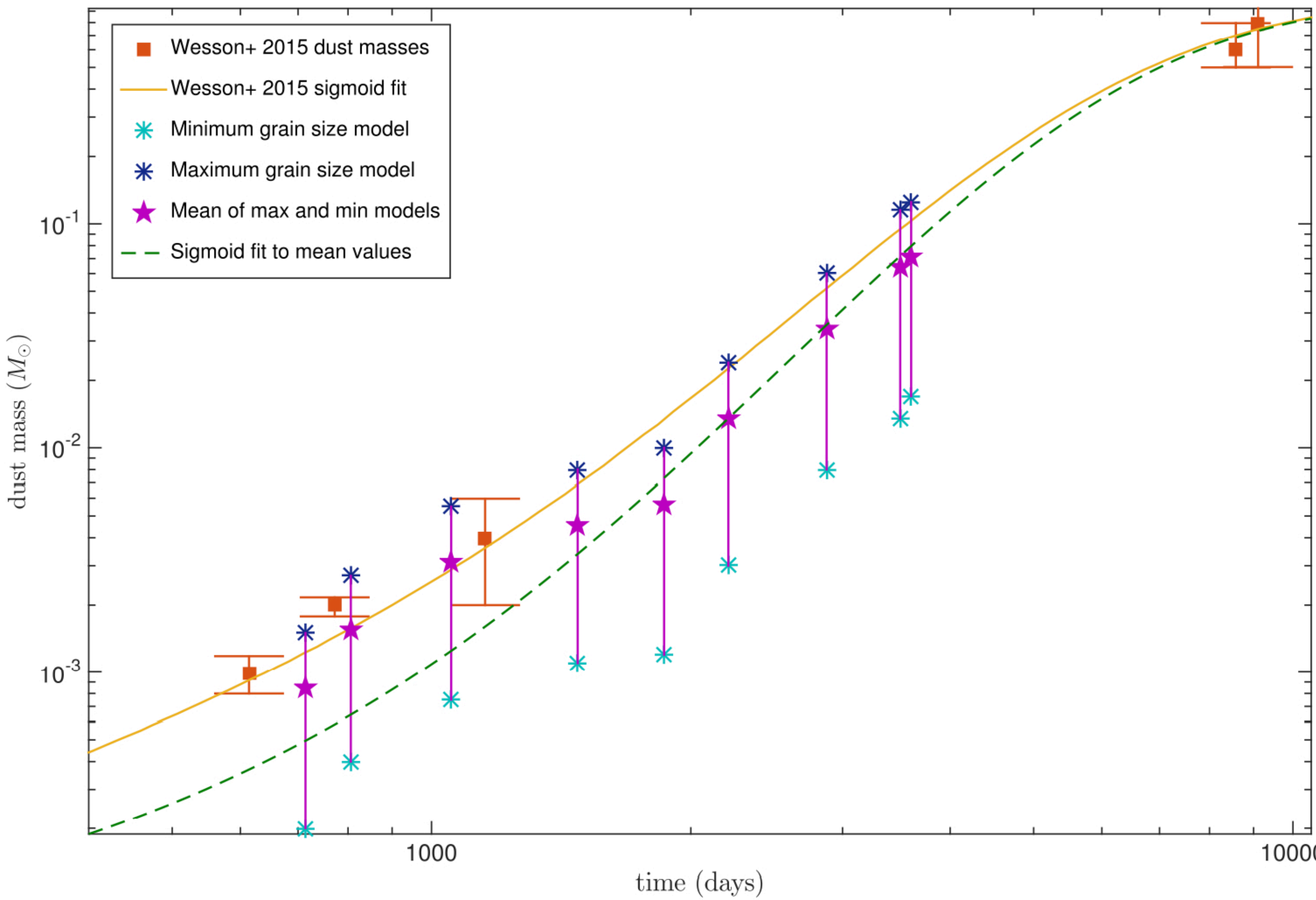

Dust in SN 1993J and Cas A

Bevan+(2017)

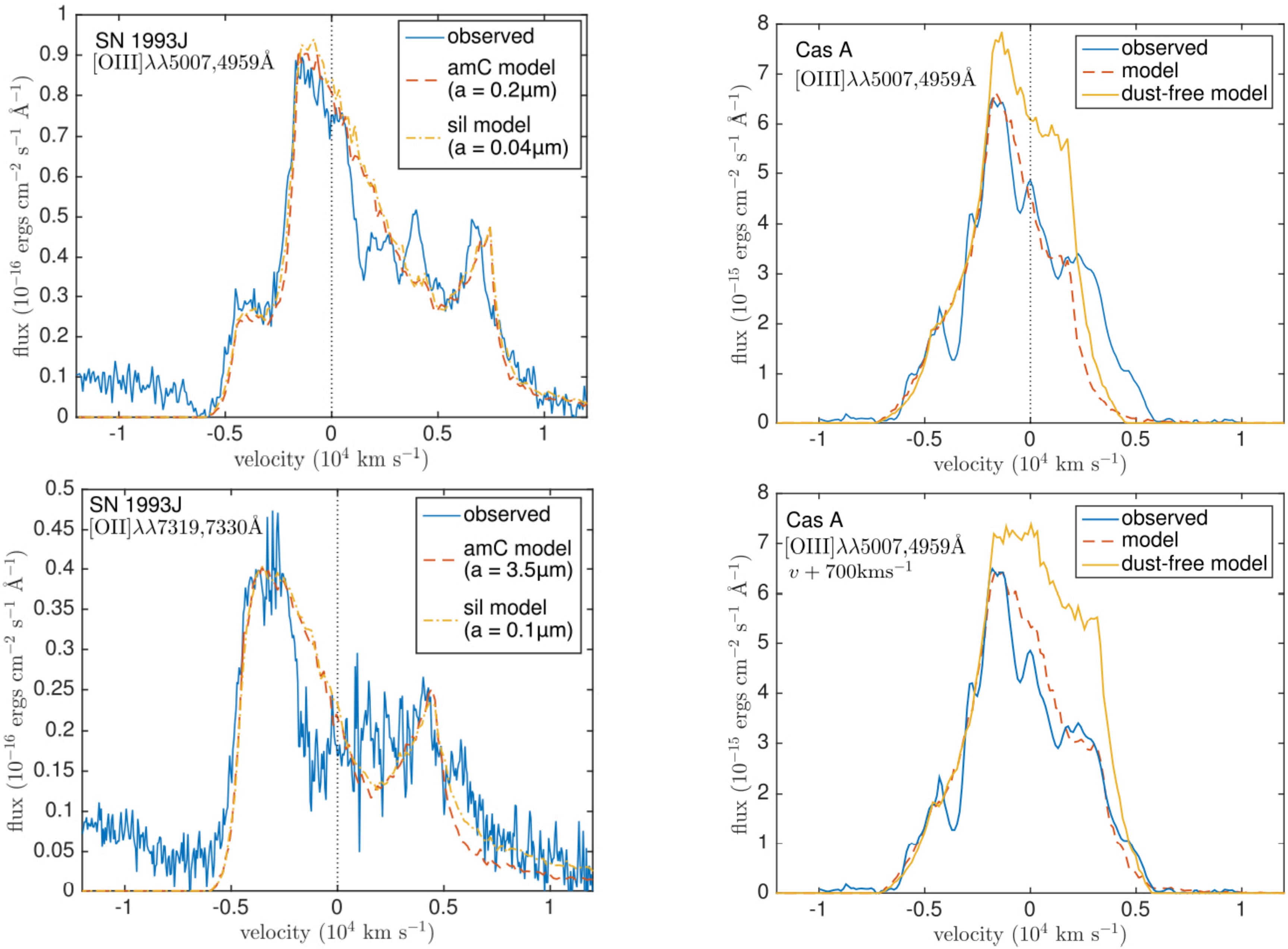

Dust in SN 1993J

Table 2. The parameters used for the smooth and clumped year 16 models for SN 1993J for media composed of 100 per cent amorphous carbon dust grains of radius 3.5 μm, or 100 per cent silicate dust grains of radius 0.1 μm. Optical depths are given from R_{in} to R_{out} at $\lambda = 7319$ Å for [O II] and $\lambda = 4959$ Å for [O III]. Smooth dust models are listed in the first four rows and clumped dust models in the last four rows.

	Clumped?	Species	a (μm)	V_{max} (km s^{-1})	V_{min} (km s^{-1})	R_{in}/R_{out}	β	R_{out} (10^{17}cm)	R_{in} (10^{17}cm)	Doublet ratio	τ_λ	f	R_{clump} (10^{17}cm)	M_{dust} ($M_\odot$)
[O III]	No	sil	0.04	6000	4500	0.75	7	3.2	2.4	2.98	0.65	–	–	0.10
[O III]	No	amC	0.2	6000	4500	0.75	7	3.2	2.4	2.98	0.63	–	–	0.005
[O II]	No	sil	0.1	6000	4500	0.75	7	3.2	2.4	1.23	0.74	–	–	0.05
[O II]	No	amC	3.5	6000	4500	0.75	7	3.2	2.4	1.23	0.60	–	–	0.12
[O III]	Yes	sil	0.04	6000	4500	0.75	7	3.2	2.4	2.98	1.00	0.1	0.13	0.15
[O III]	Yes	amC	0.2	6000	4500	0.75	7	3.2	2.4	2.98	0.96	0.1	0.13	0.008
[O II]	Yes	sil	0.1	6000	4500	0.75	7	3.2	2.4	1.23	1.12	0.1	0.13	0.08
[O II]	Yes	amC	3.5	6000	4500	0.75	7	3.2	2.4	1.23	0.95	0.1	0.13	0.18

SN 1993J is 6 years younger than SN 1987A!
Could it in following years accumulate ~1 Mo of dust?

Conclusion

1.Unknown amount of the dust present before Cas A SN explosion, and the large amount of a new dust formed after explosion give limits to the possibility of the strong constrain on the binary companion of Cas A progenitor!!!

2. The nature of CCS? What we will observe if it is a BH!?

3. Plausible existence of a CDS that contains dusty clumps enriched by Fe might explain the putative deficit of Fe in the ejecta of Cas A.

4. Simulations of SNR evolution in a clumpy CSM are needed!

Do we understand Cas A?

1. Binary companion of Cas A – yes/no?!
2. Wolfgang Kerzendorf will say more on the topic
3. Cas A remains fascinating, rich and nearby laboratory

Ways to understand SN and progenitor

1. Observations of pre-supernova field*
2. Observations of SNe Light Curves (O, IR, X, R, **γ, ν**)*
3. Observations of SNe evolution to SNR*
4. Multi-wavelength observations (O, IR, R, X, **γ**, **ν**):
 - of SNR morphology
 - element abundances of ejecta
 - search for Compact Central Source (CCS)
 - study of CCS properties
 - study of CSM properties
 - explosion energy evaluation
 - search for potential binary companion

4. Simulations of pre-supernova evolution
5. Simulations of SNe explosion
6. Simulations of SNR evolution
7. Interpretation and comparison to observations

* Not possible for Cas A